Mem. R. astr. Soc. (1975) **80**, 105–137.

OBSERVATIONS OF 31 EXTRAGALACTIC RADIO SOURCES WITH THE CAMBRIDGE 5-KM TELESCOPE AT 5 GHZ

J. M. Riley and G. G. Pooley

Mullard Radio Astronomy Observatory, Cavendish Laboratory, Cambridge

(Received 1975 July 9)

SUMMARY

Thirty-one radio sources from the 3C and 4C catalogues have been mapped with a resolution of 2″ in RA and 2″ cosec δ in Dec. The results are presented here as contour maps and in tabular form, with accurate measurements of the positions of optical objects in the fields.

1. INTRODUCTION

We present the results of observations with the 5-km telescope (Ryle 1972) of 31 extragalactic radio sources at 5 GHz. These form part of a continuing study of such objects at the Mullard Radio Astronomy Observatory (e.g. Northover 1973; Riley & Branson 1973; Hargrave & Ryle 1974; Hargrave 1974; Pooley & Henbest 1974; Turland 1975a, b; Hargrave & McEllin 1975; Longair 1975).

Most of the sources described here are in the 3CR catalogue but seven 4C sources, identified with quasars of redshift greater than 1·5 in Schmidt's (1975) sample, are also included. The positions of the optical objects associated with these sources have been measured from the prints of the National Geographic–Palomar Observatory Sky Survey to an accuracy better than 0″·75 arc.

2. THE OBSERVATIONS

The observing technique was essentially that described by Pooley & Henbest (1974) with two principal differences, namely: the polarization distributions of the sources have not been measured and the observations of most of the sources, which are of large angular extent, extended over several days. For a map made with n 12-hr observations, that is 16 n ($=N$) interferometer spacings, the first grating response of the instrument is an ellipse of semi-axes $42'' \times n$ in RA and $42'' \times n$ cosec δ in Dec. For accurate mapping of the large-scale structure, the overall angular size of a source should not exceed about half this value; there are some cases in which this condition is not satisfied and the large-scale structure should then be derived from the lower resolution maps to be found in Macdonald, Kenderdine & Neville (1968, hereafter called MKN), Mackay (1969) and Branson *et al.* (1972). In four cases (3C 83.1B, 3C 186, 3C 284 and 3C 452) grating rings due to compact components were removed numerically.

The noise level on the maps is about $3/\sqrt{n}$ mJy, and the flux density scale is based on an assumed value of 8·2 Jy for 3C 147.

3. THE RESULTS

The results are presented as contour maps in Figs 1–26 and in Table I; 1950·0 coordinates are used throughout. As the observations were made with feeds having the **E** vector in pa 90°, each contour map represents the distribution of I–Q across the source; it has been found by Pooley & Henbest (1974) that the polarization seldom exceeds 10 per cent in such sources so that an I–Q map is, in general, a reasonable representation of the distribution of the total intensity I. Each map is plotted with equal scales in RA and Dec., the angular scale being shown by an L shape and the half-power beam shape by a shaded ellipse. The contour interval for each source is indicated by the number beside the letters CI; this is the flux

density in mJy of an unresolved source which would produce a change of one contour. The brightness temperature (K) corresponding to one contour on the maps having a resolution $2'' \times 2''$ cosec δ is found by multiplying this number by 15 sin δ. For several of the very intense compact components the contours above a certain level have been omitted but the peak level is indicated. The positions of the associated optical objects are shown by crosses, the extent of each cross indicating the uncertainty in position; in all cases these are the positions measured from the Sky Survey prints using the method described in Section 4.

For six sources, 3C 83.1B, 3C 184.1, 3C 223, 3C 351, 3C 402 and 3C 452, maps at a resolution of $2'' \times 2''$ cosec δ are only given for the regions of highest brightness. In each case a lower resolution map has also been included to show the low brightness structure and to indicate the areas covered by the detailed maps. The map of 3C 28 has been convolved to a lower resolution since the whole source is of low surface brightness.

Further details of the sources are given in the figure captions. Reference is not necessarily made to the original identification or redshift determination but these may be found in earlier papers (MKN; Mackay 1969; Branson *et al.* 1972).

No maps are presented for 3C 299, 4C 38.37, 4C 21.59, 4C 29.64 and 4C 24.61 which are all of small angular size; there are notes on these sources in the footnotes to Table I.

The data for each source are presented in Table I and, in general, only the details of the more compact regions are quoted. The details of the more extensive regions may be obtained from the maps, and their flux densities by subtraction of the flux densities of the high brightness regions from the integrated flux densities.

The details in Table I are as follows:

(1) Source number from the 3C or 4C catalogues.

(2) The number of spacings, N, used in the synthesis (see Section 2).

(3), (4) 1950·0 coordinates of the peaks of emission, with estimated errors; no error is quoted if the component has no well-defined peak. The figures preceded by the word ' optical ' are the coordinates of the associated optical object measured as described in Section 4.

(5) The position angle of the major axis of the component, if well defined, after allowing for the ellipticity of the beam.

(6), (7) The angular extents of each component parallel and perpendicular to its major axis. When the component is barely resolved a gaussian brightness distribution is assumed in estimating its angular extent. For more complex components the quoted sizes are only approximate.

(8) The flux density of each component at 5 GHz with the estimated error.

(9) The overall angular extent of the source. This is usually the separation of the outermost peaks of a multiple source.

(10) The integrated flux density of the source at 5 GHz with estimated error. This is the maximum amplitude on the smallest interferometer spacing used in the observations. For 3C sources the values measured in this way agree well with those given by Kellermann, Pauliny-Toth & Williams (1969).

(11) Redshift of the associated object.

(12) Distance derived from the redshift given in column 11; an Einstein–de Sitter model has been used, assuming $H_0 = 50$ km s^{-1} Mpc^{-1}, $\Omega = 1$ and $q_0 = 0{\cdot}5$. In the case of 3C 83.1B the distance has been derived from the mean redshift of the galaxies in the Perseus cluster (Chincarini & Rood 1971).

(13) Total linear size of the source if the angular size is that given in column 9.

4. OPTICAL MEASUREMENTS

The positions of the optical objects associated with all the sources have been measured on the National Geographic–Palomar Observatory Sky Survey prints with reference to stars in the Smithsonian Catalogue. An x–y measuring machine, a Coradograph, at the Institute of Astronomy, Cambridge, was used and the data were analysed by means of a program due to A. N. Argue. A finding chart for 3C 154 is shown in Plate I. Finding charts for the other 3C sources may be found in Griffin (1963), Sandage, Véron &

Wyndham (1965), Wyndham (1966) and Spinrad & Smith (1973). Finding charts for the 4C sources are in Olsen (1970).

The accuracy of the new measurements can be estimated best by comparing where possible the positions of the optical objects with the compact central radio components which unambiguously define the nuclei of the optical identifications. There are 22 such components in the present sample and the errors in their radio positions are generally $0''{\cdot}1$–$0''{\cdot}2$ arc in RA and $0''{\cdot}1$–$0''{\cdot}2$ cosec δ in Dec., somewhat better than the expected accuracy in the optical measurements. The means of the absolute values of the differences in RA and Dec. between the optical and radio positions of the 22 objects are shown in Table II. The mean difference in RA is larger than that in Dec., but it seems likely that this apparent difference between the measurements in the two coordinates is not significant because two (3C 79 and 3C 351) of the five objects with the largest differences in RA have very weak central radio components, one (3C 299) is extremely faint optically and one (3C 83.1B) is a large galaxy whose centre is difficult to measure on the Sky Survey prints. For the whole sample the largest deviations between the radio and optical positions occur when the optical object is very close to the edge of the Sky Survey print, when it is almost at the plate limit or when the reference stars are very unevenly distributed around it.

Our optical measurements are also compared in Table II with those of other authors for the few objects which have been measured with accuracies better than $\approx 0''{\cdot}75$ arc; the results agree within the errors quoted.

TABLE II

	No. of sources	Mean differences ($''$) α	δ
Present optical—Radio	22	0·60	0·42
Murray *et al.* (1969)	1	0·33	0·18
Argue & Kenworthy (1972)	1	0·21	0·17
Griffin (1963)	1	0·20	0·52
Barbieri *et al.* (1970)	1	0·32	0·68
Wall (1973)	1	1·49	1·1

ACKNOWLEDGMENTS

We thank the many members of staff of the Observatory for their work in the operation of the telescope, and Mr A. N. Argue for the use of the x–y measuring machine. JMR thanks Newnham College, Cambridge, for a Research Fellowship.

REFERENCES

Argue, A. N. & Kenworthy, C. M., 1972. *Mon. Not. R. astr. Soc.*, **160,** 197.
Barbieri, C., Capaccioli, M. & Pinto, G., 1970. *Mem. Soc. astr. Ital.*, **41,** 459.
Branson, N. J. B. A., Elsmore, B., Pooley, G. G. & Ryle, M., 1972. *Mon. Not. R. astr. Soc.*, **156,** 377.
Chincarini, G. & Rood, H. J., 1971. *Astrophys. J.*, **168,** 321.
Griffin, R. F., 1963. *Astr. J.*, **68,** 421.
Hargrave, P. J., 1974. *Mon. Not. R. astr. Soc.*, **168,** 491.
Hargrave, P. J. & McEllin, M., 1975. *Mon. Not. R. astr. Soc.*, **173,** 37.
Hargrave, P. J. & Ryle, M., 1974. *Mon. Not. R. astr. Soc.*, **166,** 305.
Kapahi, V. K., Gopal-Krishna & Joshi, M. N., 1974. *Mon. Not. R. astr. Soc.*, **167,** 299.
Kellermann, K. I., Pauliny-Toth, I. I. K. & Williams, P. J. S., 1969. *Astrophys. J.*, **157,** 1.
Kristian, J., Sandage, A. & Katem, B., 1974. *Astrophys. J.*, **191,** 43.
Longair, M. S., 1975. *Mon. Not. R. astr. Soc.*, **173,** 309.
Macdonald, G. H., Kenderdine, S. & Neville, A. C., 1968. *Mon. Not. R. astr. Soc.*, **138,** 259.
Mackay, C. D., 1969. *Mon. Not. R. astr. Soc.*, **145,** 31.
Murray, C. A., Tucker, R. H. & Clements, E. D., 1969. *Nature*, **221,** 1229.
Northover, K. J. E., 1973. *Mon. Not. R. astr. Soc.*, **165,** 369.
Olsen, E. T., 1970. *Astr. J.*, **75,** 764.
Pooley, G. G. & Henbest, S. N., 1974. *Mon. Not. R. astr. Soc.*, **169,** 477.
Riley, J. M. & Branson, N. J. B. A., 1973. *Mon. Not. R. astr. Soc.*, **164,** 271.

Ryle, M., 1972. *Nature*, **239,** 435.
Ryle, M. & Windram, M. D., 1968. *Mon. Not. R. astr. Soc.*, **138,** 1.
Sandage, A. R., Véron, P. & Wyndham, J. D., 1965. *Astrophys. J.*, **142,** 1307.
Schmidt, M., 1975. *Astrophys. J.*, **195,** 253.
Spinrad, H. & Smith, H. E., 1973. *Astrophys. J.*, **179,** L71.
Turland, B. D., 1975a. *Mon. Not. R. astr. Soc.*, **170,** 281.
Turland, B. D., 1975b. *Mon. Not. R. astr. Soc.*, **172,** 181.
Wall, J. V., 1973. *Astrophys. Lett.*, **15,** 101.
Wellington, K. J., Miley, G. K. & van der Laan, H., 1973. *Nature*, **244,** 502.
Wilkinson, P. N., Richards, P. J. & Bowden, T. N., 1974. *Mon. Not. R. astr. Soc.*, **168,** 515.
Wyndham, J. D., 1966. *Astrophys. J.*, **144,** 459.

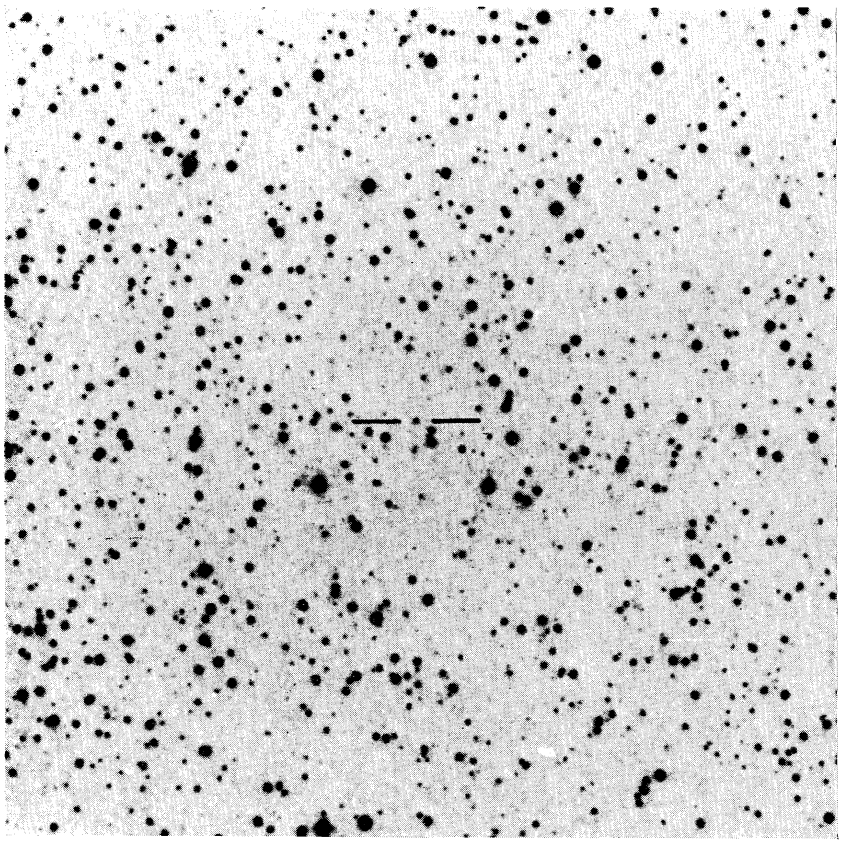

PLATE I. *Finding chart for* 3C 154*; the field is* 15 × 15 *arcmin. North is to the top and east to the left. This is taken from the blue print of the Sky Survey.* (© 1957 *National Geographic–Palomar Observatory Sky Survey.*)

[*facing page* 108]

TABLE 1

Source 3C	N	RA h m s	± s	Dec. ′ ″	± ″	pa	Component ω_{max} ″	ω_{min} ″	Flux density mJy	±	θ ″	Integrated flux density mJy	±	z	Distance Mpc	Total size kpc
28	32	00 53 08.4	–	26 08 33	–	–	5	5	130	50	30	300	50	0.1959	1030	140
		09.5	–	09	–	–	8	5	220	50						
Optical		09.10	0.06	22.6	0.5											
79	64	03 07 08.933	0.007	16 54 50.0	0.4	126	4.3	1.8	240	20	87	1400	100	0.2561	1290	430
		11.35	0.02	36.8	1.0	–	< 7	< 2	12	5						
		14.744	0.007	27.1	0.4	90	4.7	1.9	170	20						
Optical		11.48	0.05	36.9	0.9											
83.1B	48	03 14 56.79	0.02	41 40 32.6	0.3	–	< 0.8	< 0.5	21	3	200	–	–	0.0256	108	100
Optical		56.92	0.10	33.0	1.0											
109	32	04 10 53.37	0.01	11 05 16.7	0.7	142	10	7	360	80	90	1700	200	0.3056	1500	500
		54.850	0.007	04 39.5	0.5	–	< 8	< 0.5	320	30						
		57.030	0.007	04.1	0.5	110	8	2.3	410	60						
Optical		54.87	0.05	41.4	0.5											
154	32	06 10 42.50	0.05	26 05 31	1	90	4	3	1160	300	50	2250	500	–	–	–
		43.720	0.007	30.2	0.2	–	< 4	< 0.5	540	50						
		46.06	0.01	23.7	0.3	–	< 4.5	< 2	70	20						
Optical		43.79	0.05	30.1	0.5											
184.1	64	07 34 05.0	–	80 34 54.8	–	0	4	3.8	180	50	167	1300	100	0.1187	650	470
		25.1	0.1	33 24.6	0.3	–	< 2	< 2	6	3						
		34.8	0.1	32 11.1	0.3	0	5	2	160	50						
Optical		25.09	0.4	33 24.4	0.7											
186	16	07 40 56.78	0.01	38 00 30.9	0.2	148	2.7	0.8	340	20	100	380	70	1.063	3650	860
		41 00.34	0.02	37 58 59.8	0.3	–	< 1.5	< 1.0	35	7						
Optical		40 56.77	0.06	38 00 30.9	0.6											
197.1	16	08 18 00.88	0.02	47 12 02.5	0.3	15	2.5	2	380	80	14	640	70	0.1302	710	41
		00.88	0.03	16.0	0.5	–	7	3	460	100						
Optical		00.79	0.08	11.9	0.6											
223	64	09 36 47.4	–	36 09 49	–	–	12	8	500	100	250	1500	100	0.1367	740	920
		50.86	0.03	07 34.7	0.7	–	< 3.5	< 2.0	9	3						
Optical		50.82	0.08	07 35.0	0.5											
223.1	32	09 38 17.48	0.02	39 57 47.0	0.3	90	5.6	3.6	320	50	76	580	60	0.1075	600	200
		19.18	0.02	59 00.2	0.3	130	3	2.2	390	60						
Optical		18.33	0.06	58 22.2	0.7											

TABLE 1—*continued*

Source 3C/4C	N	RA h m s	± s	Dec. ° ′ ″	± ″	pa	Component ω_{max} ″	ω_{min} ″	Flux density mJy	±	θ ″	Integrated flux density mJy	±	z	Distance Mpc	Total size kpc
234	64	09 58 53.985	0.008	29 01 22.9	0.2	72	2.6	1.8	500	70	110	1900	200	0.1846	970	440
		58 57.375	0.008	01 37.4	0.2	–	< 2	< 1	90	10						
		59 01.663	0.008	02 07.3	0.2	70	2.3	1.4	230	40						
Optical		58 57.40	0.06	01 37.9	0.6											
268.2	32	11 58 23.81	0.02	31 49 19.0	0.4	90	3.6	2	90	20	96	480	50	0.361	1710	580
		26.24	0.02	31 50 50.0	0.4	90	6	5	160	40						
Optical		24.86	0.06	05.4	0.9											
284	64	13 08 33.680	0.010	27 44 22.0	0.3	0	3.5	1.5	40	10	175	640	100	0.2394	1220	840
		46.639	0.007	43 47.1	0.2	0	3.8	1.4	130	15						
Optical		41.33	0.07	44 02.6	0.6											
299[1]	16	14 19 06.403	0.004	41 58 30.37	0.07	–	< 1.0	< 0.6	1000	80	–	1000	80	0.367	1740	< 6
		05.46	0.05	25.6	0.5	–	3	2	60	30						
Optical		06.29	0.10	30.2	1.0											
300	32	14 20 36.6	–	19 49 57	–	137	18	4	160	30	96	1250	80	0.272	1360	500
		39.93	0.01	49 13.3	0.6	–	< 2	< 6	9	3						
		40.8	–	48 49	–	–	12	8	550	100						
		41.500	0.007	48 54.2	0.3	–	≤ 3.4	≤ 2.2	390	40						
Optical		39.96	0.06	49 13.2	0.6											
332	32	16 15 46.1	–	32 29 17	–	–	10	10	460	90	80	1050	80	0.152	820	280
		46.97	0.02	29 50.3	0.4	22	3.5	< 2	26	6						
		47.42	0.02	30 23.6	0.4	–	10	10	430	90						
Optical		46.95	0.05	29 51.0	0.6											
351	32	17 04 01.5	–	60 48 04	–	–	–	–	≈ 200	100	58	1250	60	0.371	1750	370
		03.55	0.03	31.2	0.2	–	< 2	< 2	15	5						
		05.64	0.01	53.5	0.1	0	1.5	1.2	620	60						
		05.95	0.01	48.8	0.1	168	1.5	1	340	40						
Optical		03.35	0.10	30.6	0.5											
357	32	17 26 24.86	0.02	31 48 26.0	0.4	–	9	4	290	60	80	1000	100	0.1670	890	310
		30.91	0.02	09.5	0.4	–	9	6	280	60						
Optical		27.24	0.07	24.8	0.5											
381	32	18 32 24.14	0.02	47 24 02.1	0.4	25	6	3	430	50	69	1600	100	0.1614	860	250
		24.650	0.010	25 11.0	0.1	–	< 1.5	< 1	390	40						
Optical		24.47	0.07	24 39.0	0.6											
402	64	19 40 21.81	0.03	50 30 49.1	0.3	–	2	< 2	18	4	250	800	50	0.0247	150	300
		25.55	0.02	28 37.9	0.2	–	≤ 1.5	< 1	45	5						
Optical		21.82	0.15	30 49.8	1.0											
		25.65	0.15	28 38.4	1.0											

1975MNRAS.170..105R

430	32	21 16	59.23	0.03	60 34	54.7	0.2	90	4	1	240	40	85	3200	200	0.0549	330	120
		17	02.74	0.03	35	26.4	0.2	–	< 1.1	< 1	20	5						
			05.80	0.03	36	03.7	0.2	90	5	2	380	60						
	Optical		02.75	0.15	35	26.0	0.7											
436	32	21 41	57.85	0.03	27 57	26.1	0.8	90	6	< 1	50	10	104	1000	100	0.2154	1110	460
			57.95	0.02	56	30.1	0.4	–	< 4	< 1	19	4						
			58.34	0.03	55	42.8	0.8	–	6	3	210	40						
	Optical		57.91	0.06	56	30.3	0.6											
452	16	22 43	21.64	0.02	39 25	10.5	0.3	–	7	12	300	60	250	–	–	0.0820	460	520
			32.81	0.01		27.6	0.2	–	< 0.8	< 0.5	130	20						
			43.4	–		58	–	–	13	11	230	50						
	Optical		32.79	0.06		27.3	0.5											
470	16	23 56	02.30	0.02	43 47	56.2	0.3	30	2.6	≤ 1	590	60	24	600	60	–	–	–
			03.66	0.02	48	15.0	0.3	–	< 2	< 3	70	10						
	Optical		02.67	0.07	48	13.4	0.5											
			02.88	0.07	47	58.2	0.5											
29.01	16	00 51	02.07	0.02	29 08	51.1	0.4	61	2.9	2	350	70	–	350	70	1.828	4860	24
	Optical		02.09	0.05		51.7	0.5											
25.21	16	07 30	05.20	0.02	25 42	57.1	0.5	136	10	< 1.5	250	50	–	250	50	2.686	5750	76
	Optical		05.40	0.05		55.4	0.5											
38.37[2]	16	13 43	26.582	0.004	38 38	11.79	0.08	–	< 0.8	< 0.5	440	20	–	440	20	1.844	4880	< 7
	Optical		26.55	0.06		12.0	0.5											
28.40	16	16 06	09.316	0.007	28 57	07.0	0.2	–	< 2	< 1	75	8	30	160	30	1.989	5060	250
			10.74	0.02	56	43.3	0.4	0	3	1.7	75	20						
	Optical		09.95	0.06		55.1	0.7											
21.59[3]	16	21 49	26.090	0.004	21 16	06.90	0.14	–	< 1.4	< 0.5	400	20	–	400	20	1.534	4460	<12
	Optical		26.11	0.05		06.9	0.5											
29.64[4]	16	21 56	27.704	0.004	29 44	45.78	0.10	–	< 1.4	< 0.5	490	20	–	490	20	1.753	4770	<12
	Optical		27.72	0.06		46.1	0.6											
24.61[5]	16	22 51	44.408	0.004	24 29	23.76	0.12	–	< 1.3	< 0.5	820	20	–	820	20	2.328	5420	<10
	Optical		44.32	0.05		24.7	0.5											

Footnotes:

1. 19[m] double galaxy, apparently lying in a cluster, is coincident with the bright radio component; there is possibly a weak radio component 11″ arc to the south-west. The position of the galaxy has also been measured by Kristian *et al.* (1974).
2. 18[m] quasar.
3. 19[m] quasar.
4. 20[m] quasar.
5. 18[m] quasar. The position of the quasar has also been measured by Wall (1973).

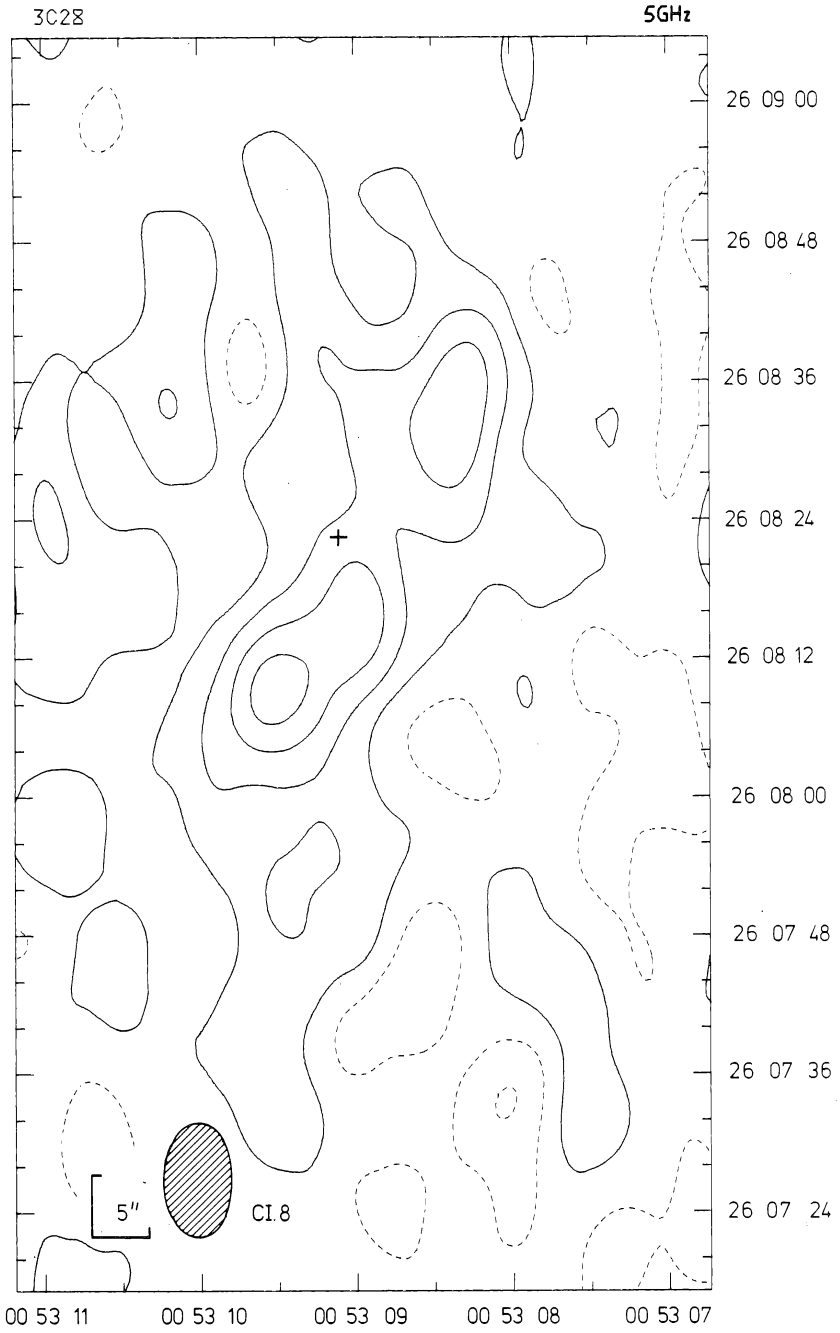

FIG. 1. 3C 28. *This map has been smoothed to a resolution of* 6″ × 10″. *There is no structure on a scale less than* 2″ × 4″ *brighter than* 15 m*Jy. The* 18^{m} *galaxy in the cluster Abell* 115 *is marked.*

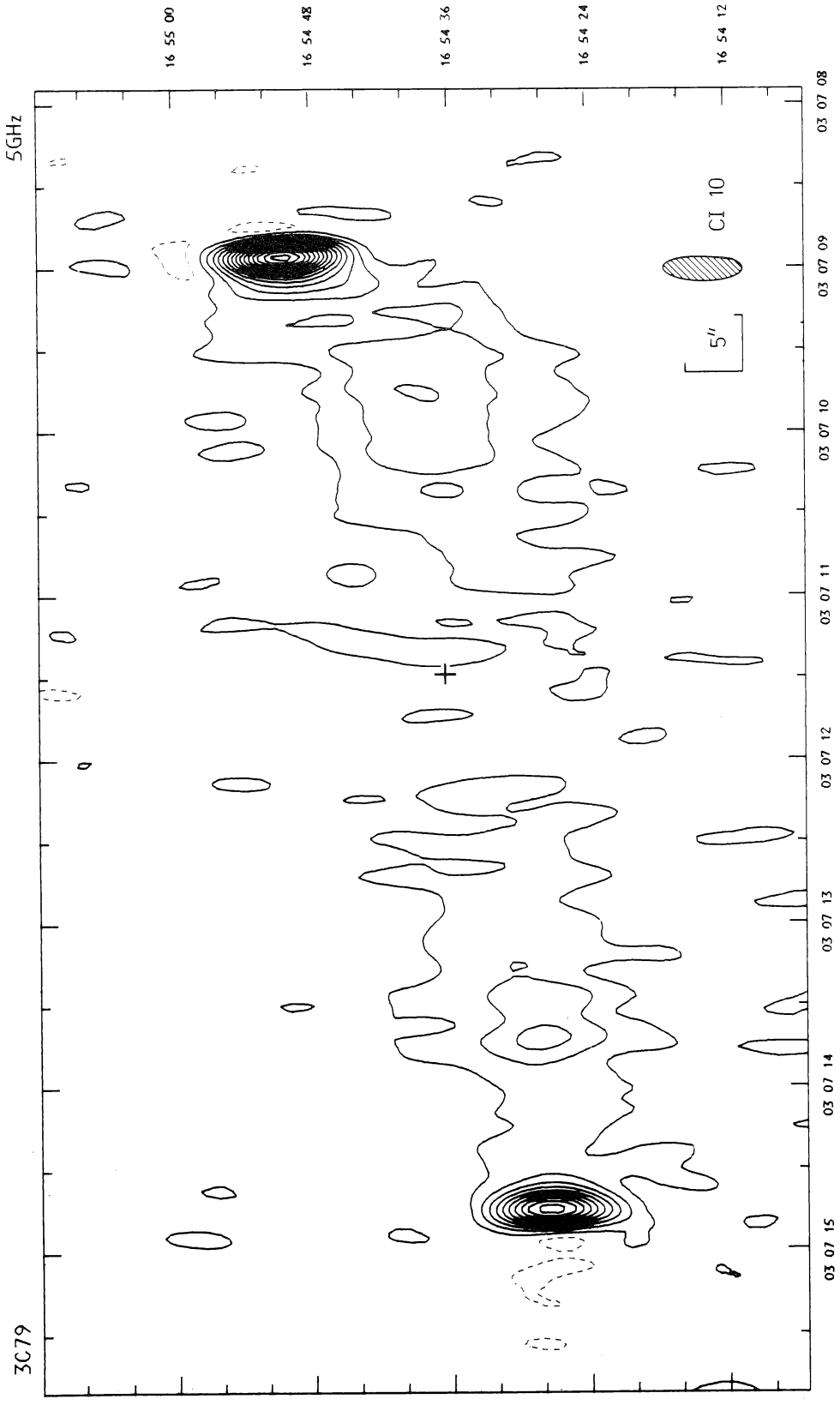

FIG. 2. *3C 79. A very weak radio component lies close to the 18^{m} galaxy.*

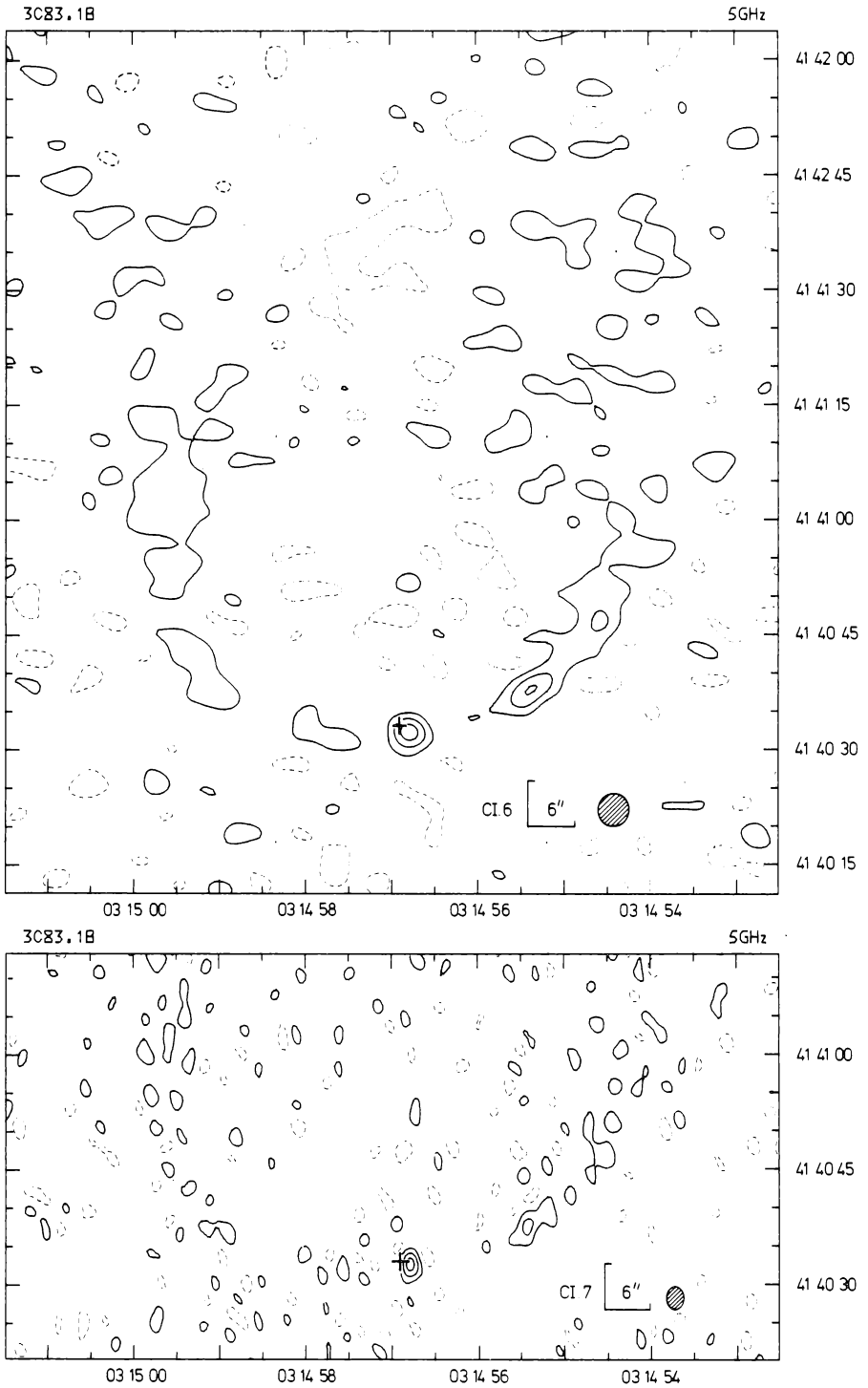

FIG. 3. 3C 83.1B. *The larger map shows the source at a resolution* 4″·5 × 4″·5, *indicating the low-brightness structure, and the smaller map is at the full resolution* (2″ × 3″). *The cross marks the position of the centre of NGC* 1265, *a* 14^m *galaxy in the Perseus cluster. See Ryle & Windram* (1968) *and Wellington, Miley & van der Laan* (1973).

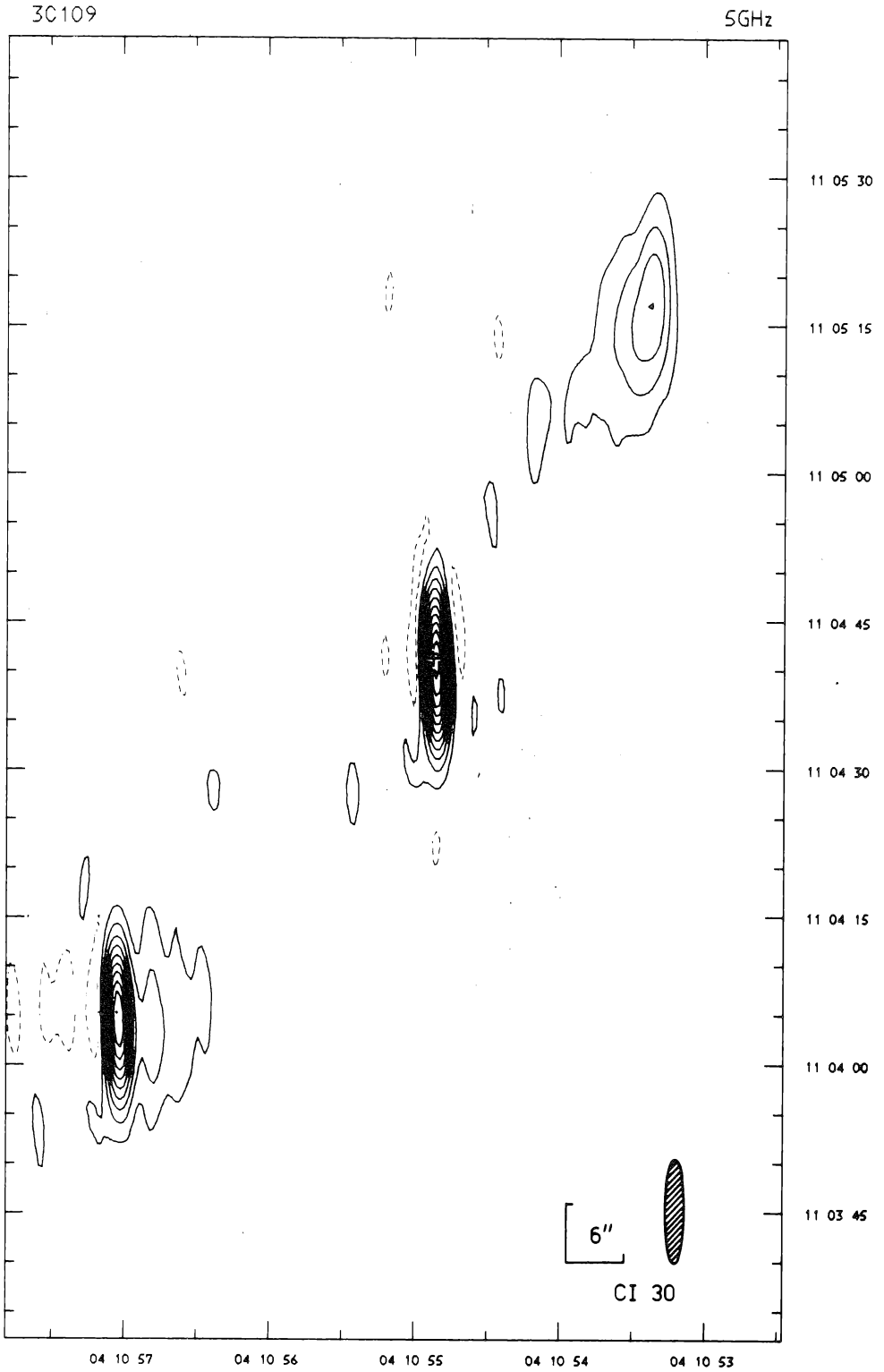

FIG. 4. 3*C* 109. *The cross marks the position of a* 16^m *N galaxy.*

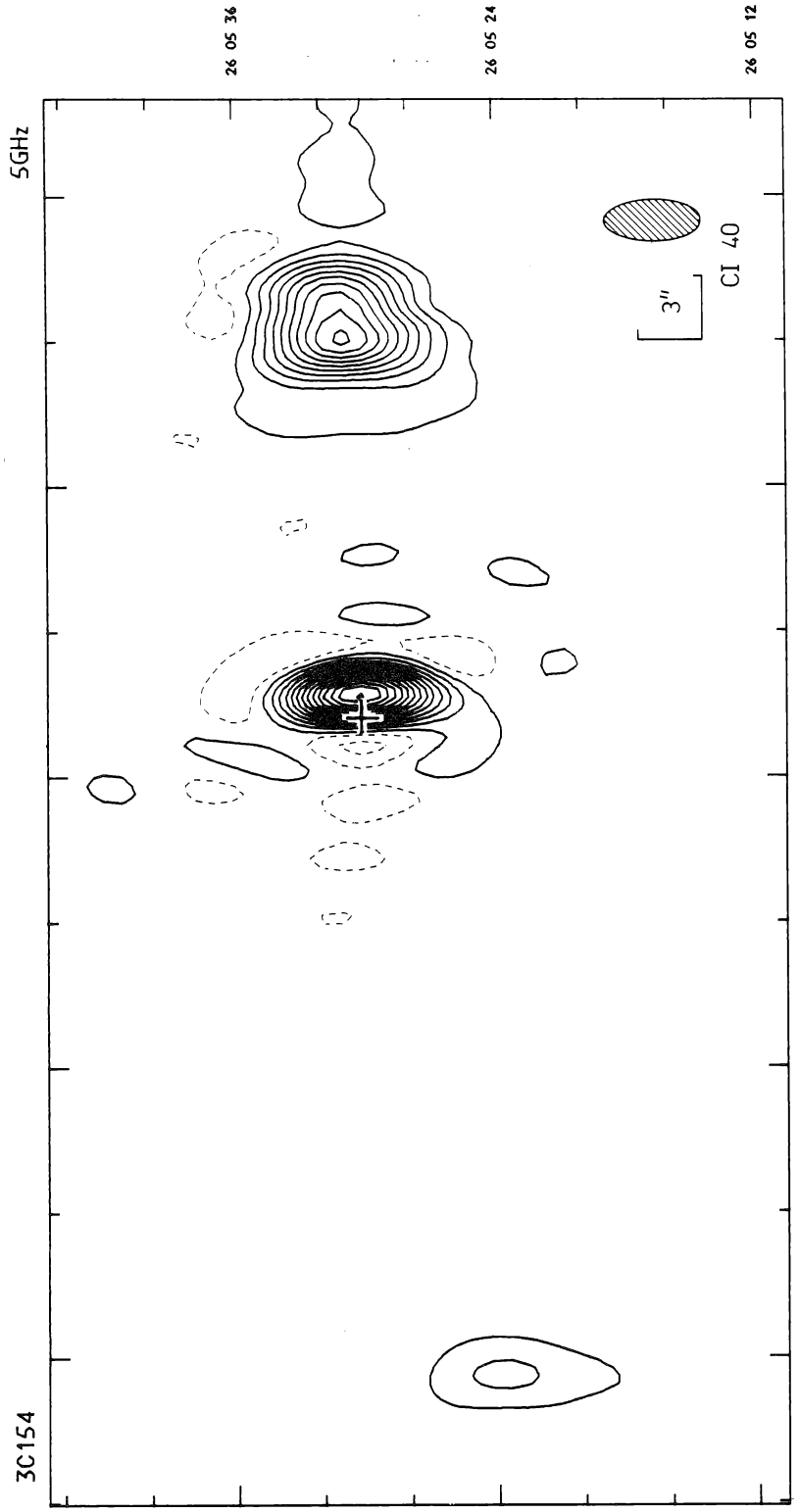

FIG. 5. 3C 154. *The* 19^m *optical object marked is shown in the finding chart (Plate I) and is object* 4 *of Kapahi, Gopal-Krishna & Joshi* (1974).

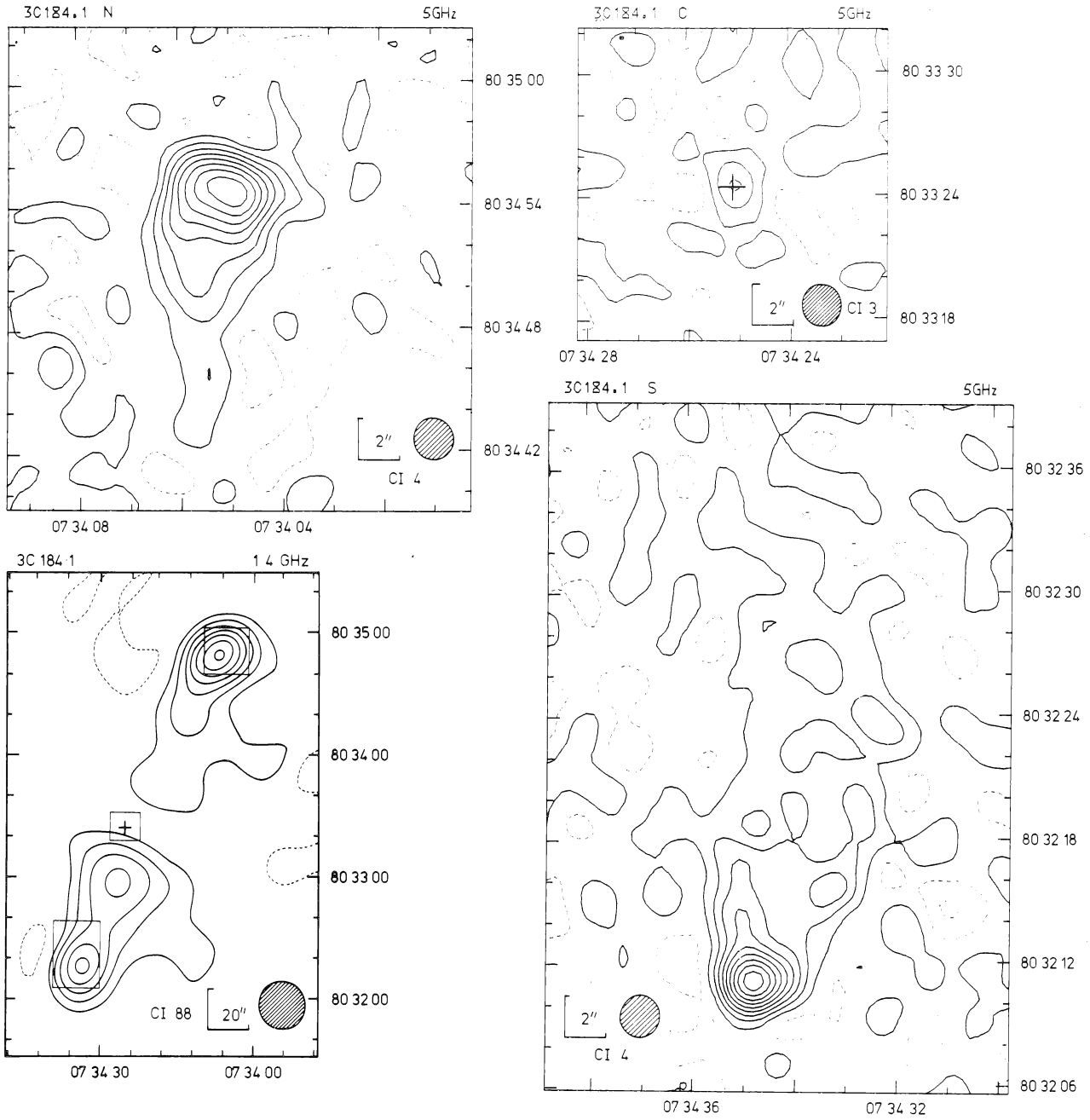

FIG. 6. *3C 184.1. High-resolution maps of three components are shown separately. The map made at 1·4 GHz with the One-Mile telescope (MKN) shows the relative positions of these areas. The identification marked is a 17^m galaxy, object* a *of MKN (wrongly positioned in that paper).*

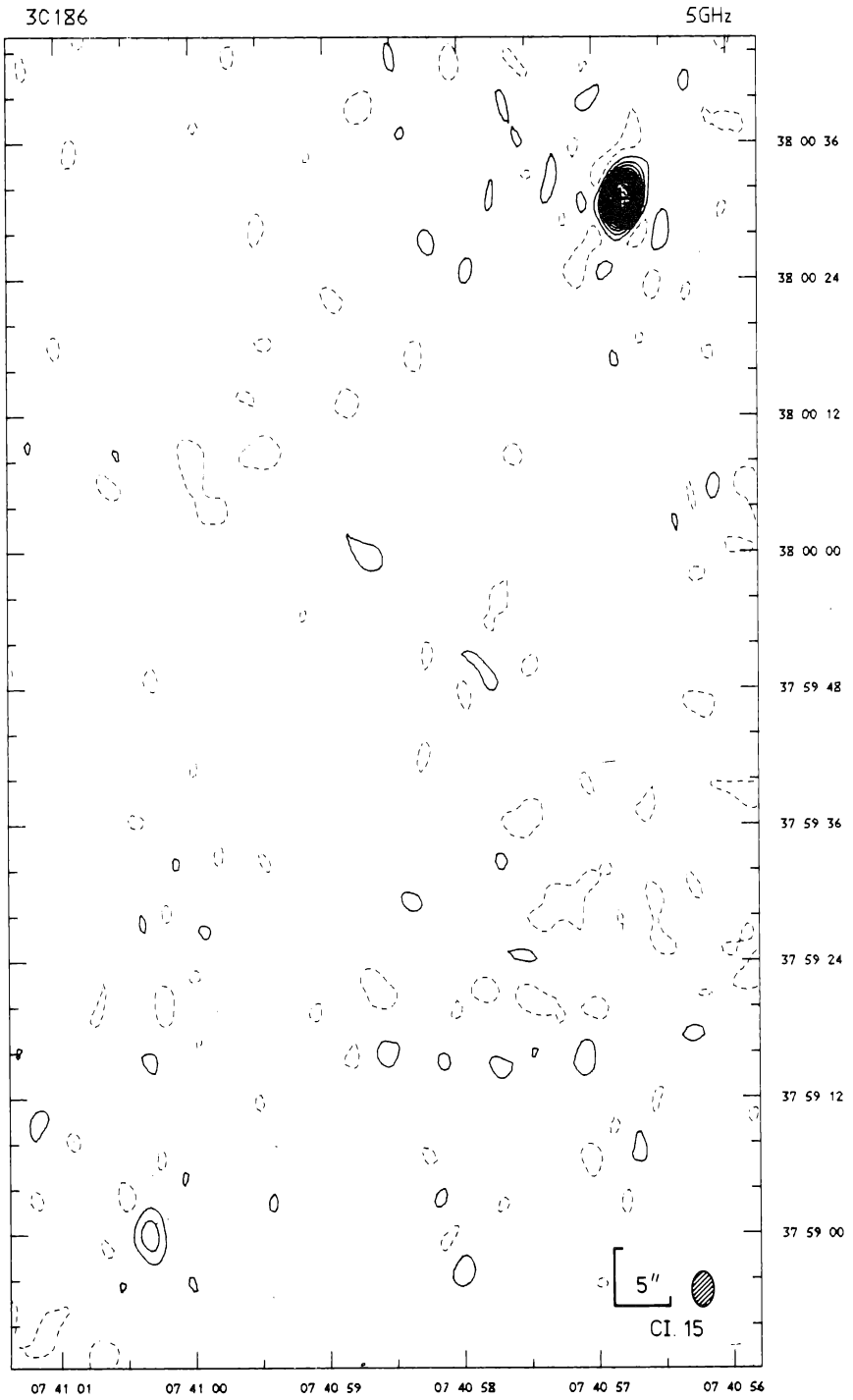

FIG. 7. 3C 186. *The cross marks a* $17^{m}{\cdot}6$ *quasar; the position of this object has also been measured by Murray, Tucker & Clements* (1969) *and Argue & Kenworthy* (1972).

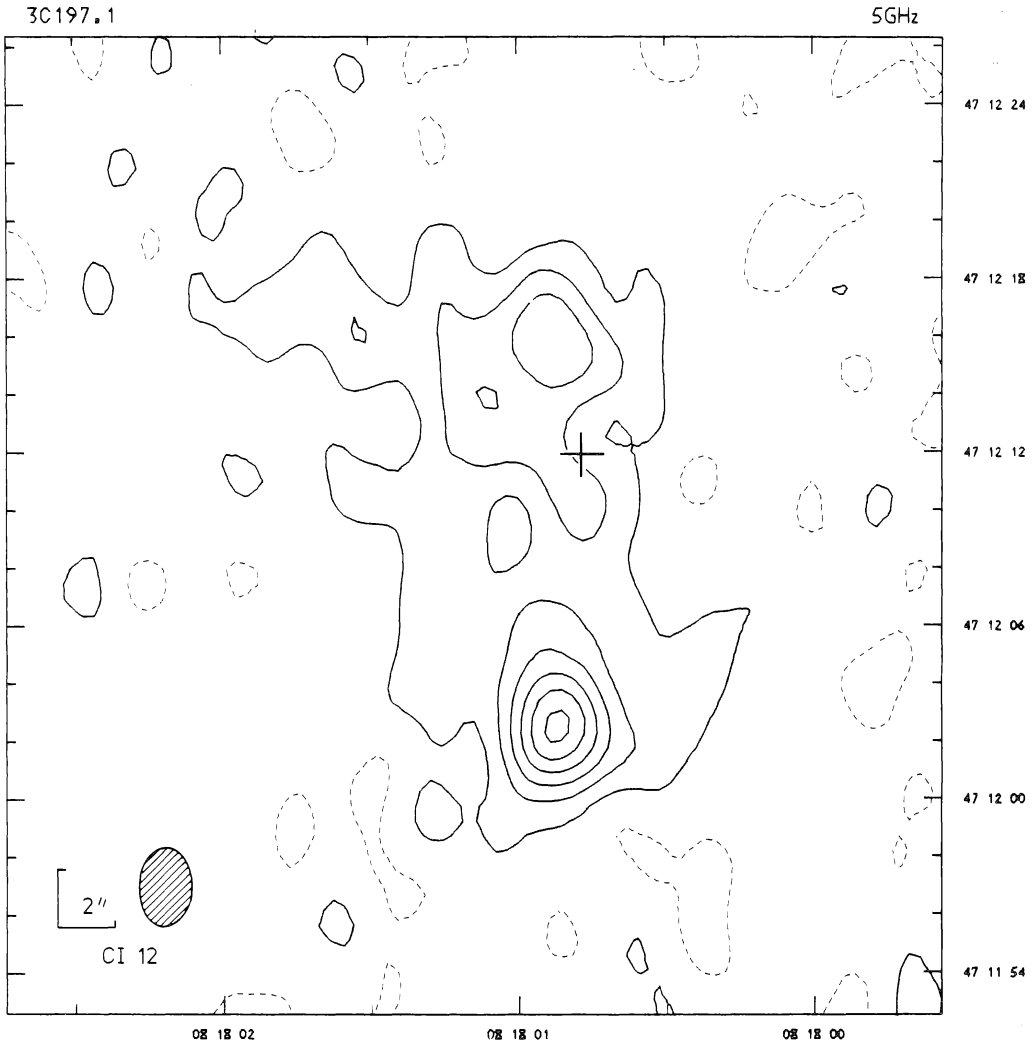

FIG. 8. *3C 197.1. The cross marks a 17^m galaxy which lies in a small group.*

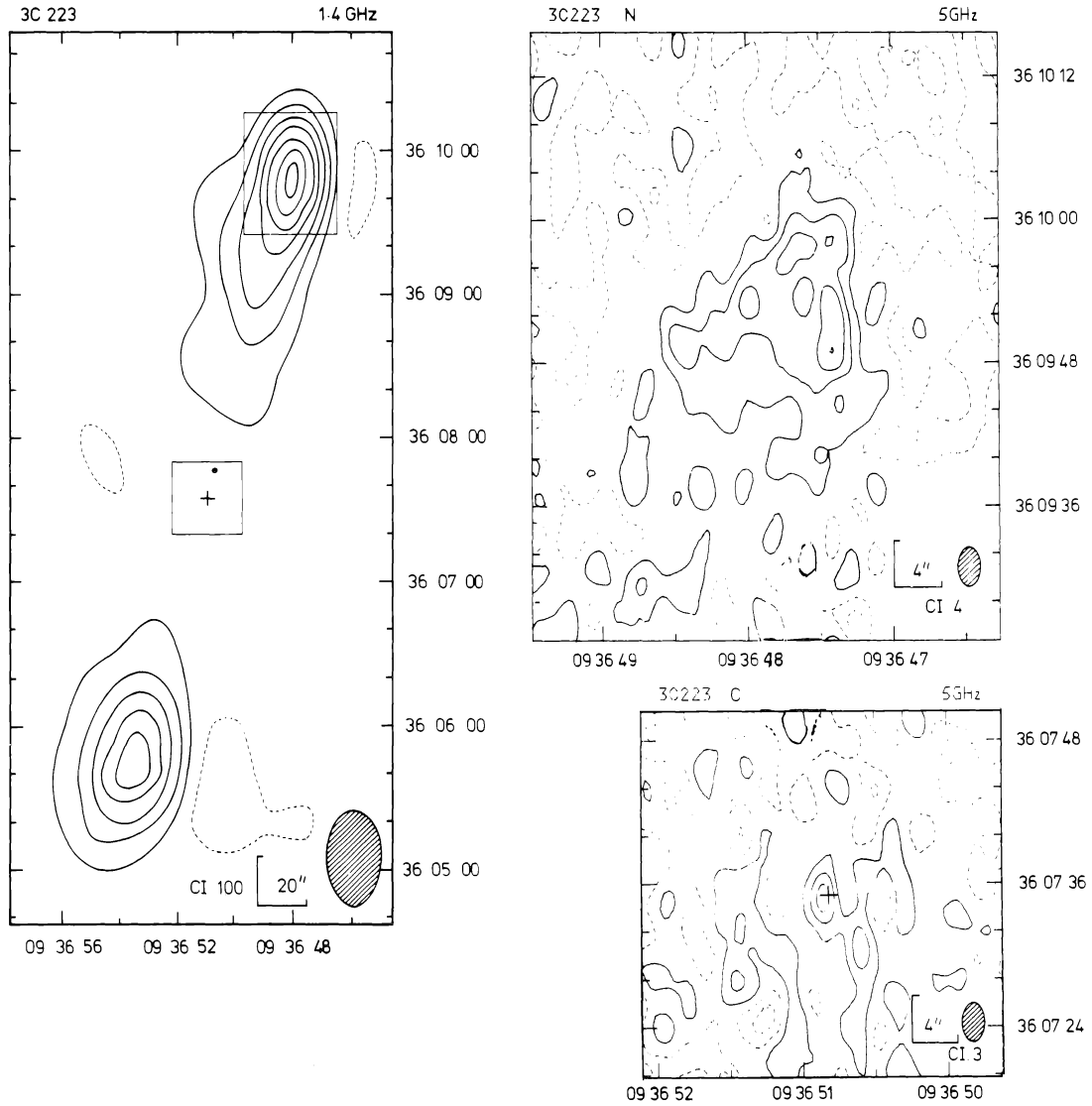

FIG. 9. 3C 223. *The overall structure of the source is shown on the 1·4 GHz map from Mackay (1969). The detailed maps of the northern and central components are shown separately. The cross marks a* 17^m *galaxy which lies in a small group.*

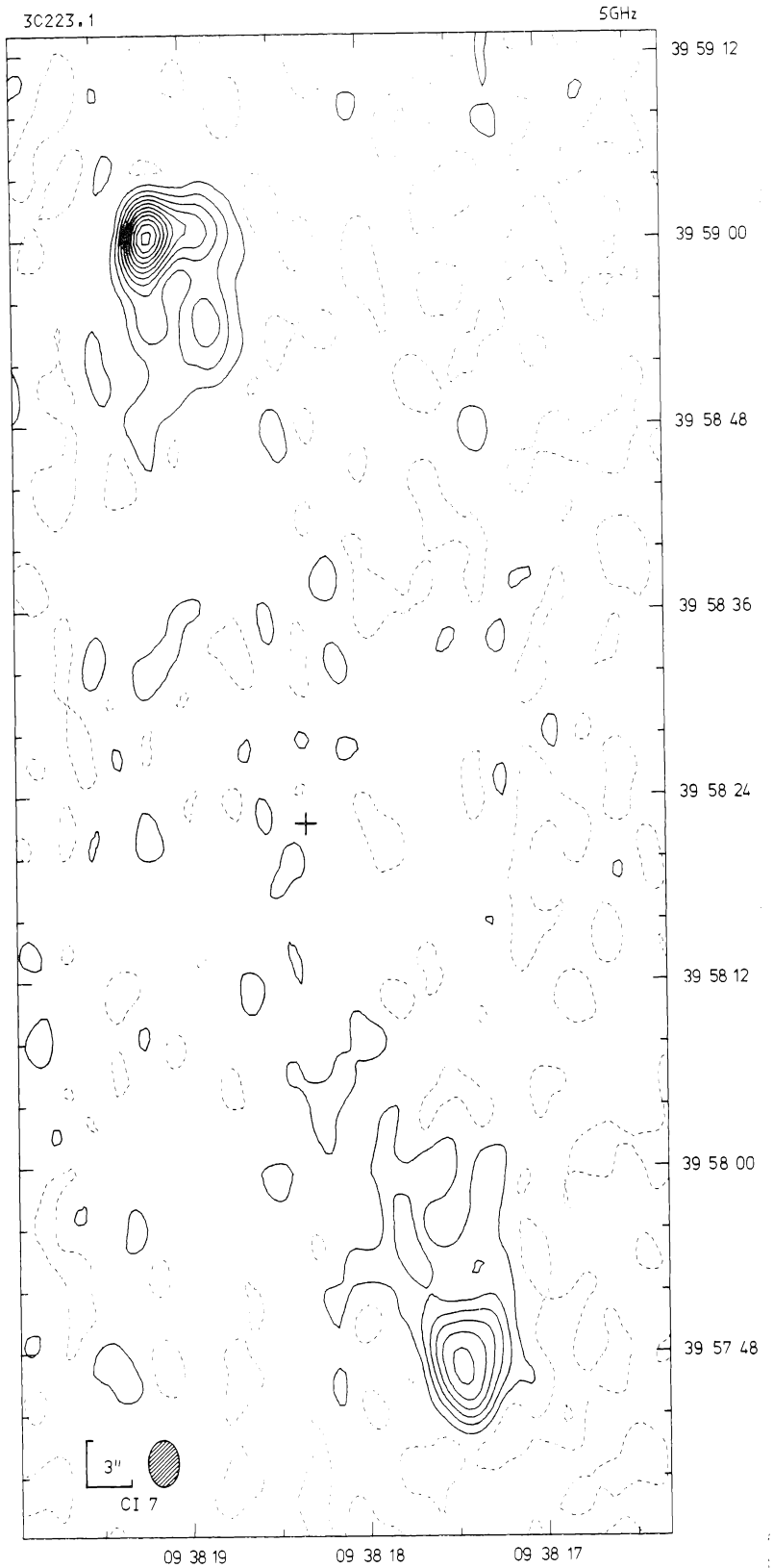

FIG. 10. 3C 223.1: *The cross marks the position of a* 16^m *elliptical galaxy (the position is wrongly shown in MKN).*

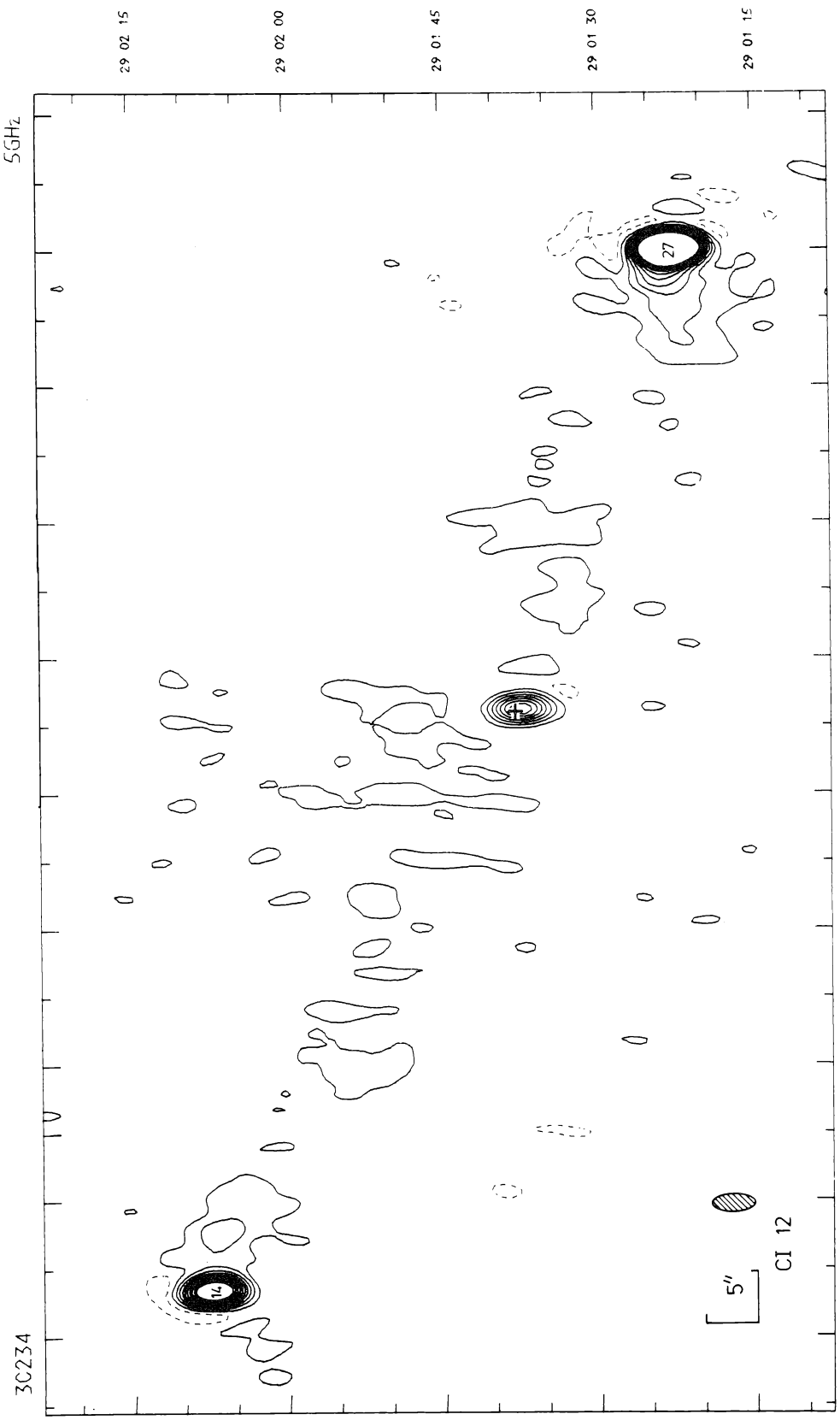

FIG. 11. *3C 234. The cross marks a* $17^m{\cdot}5$ *N galaxy, lying in a group; the position of this object has also been measured by Griffin* (1963).

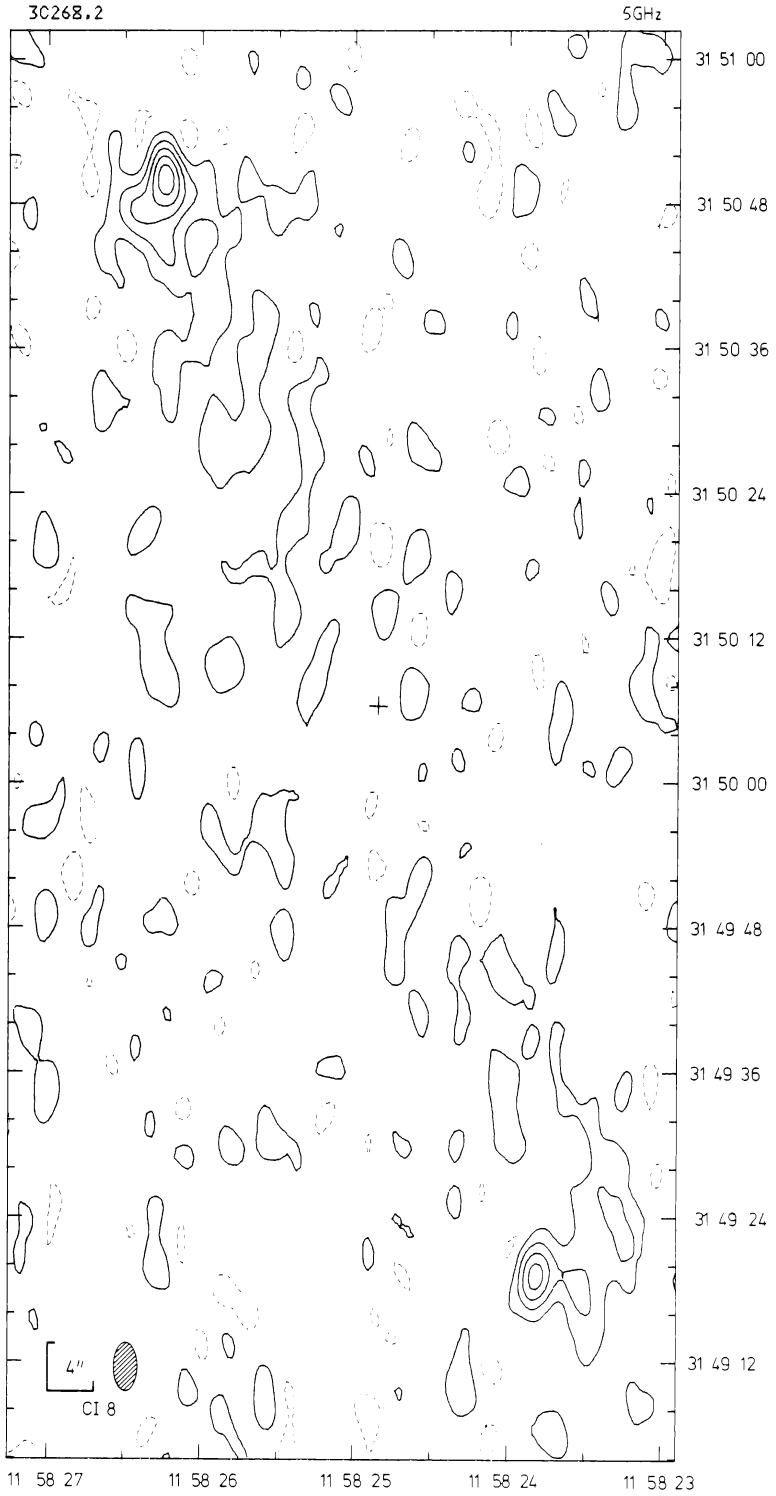

FIG. 12. 3C 268.2. *The cross marks the position of a* 19^m *galaxy of redshift* 0·361 (*Spinrad, private communication*).

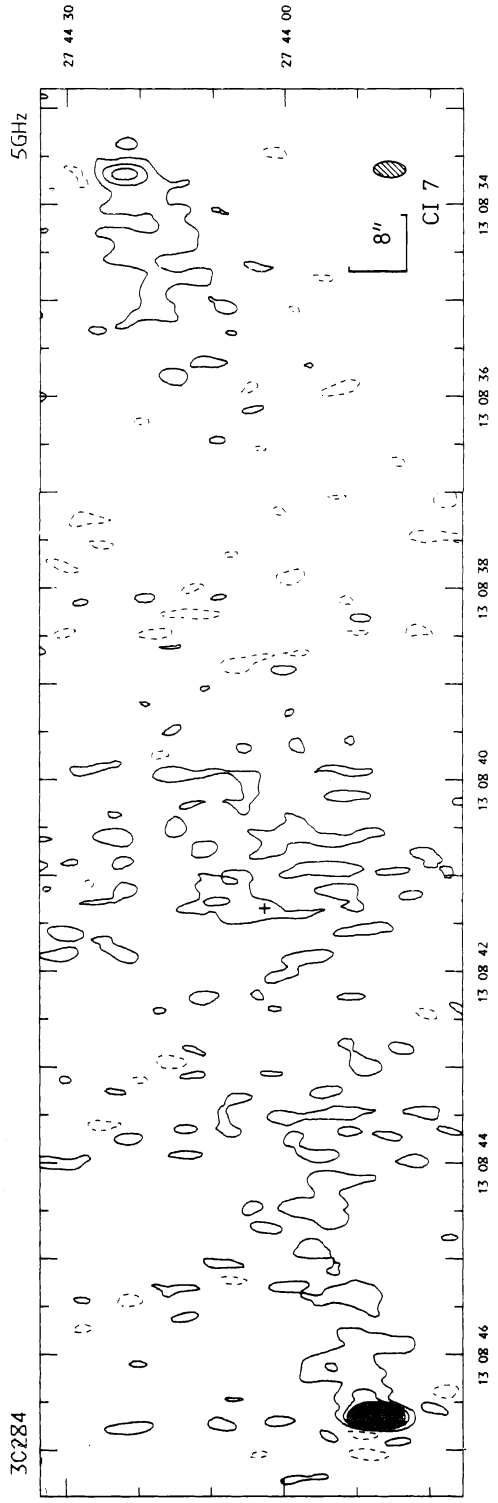

FIG. 13. *3C 284. The cross marks the position of an* 18^m *red galaxy in a cluster.*

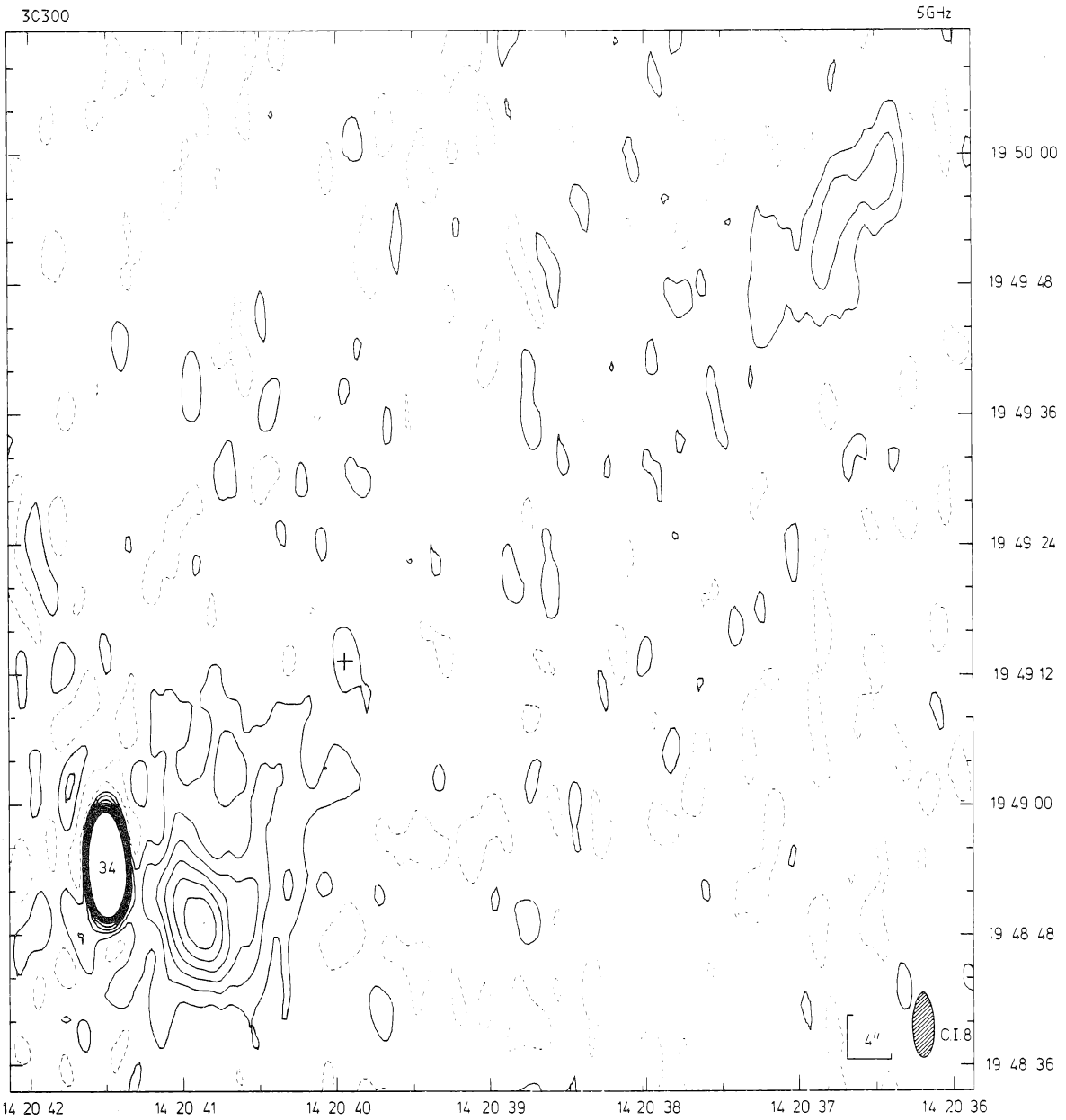

FIG. 14. 3*C* 300. *The cross marks an* 18^m *very red galaxy.*

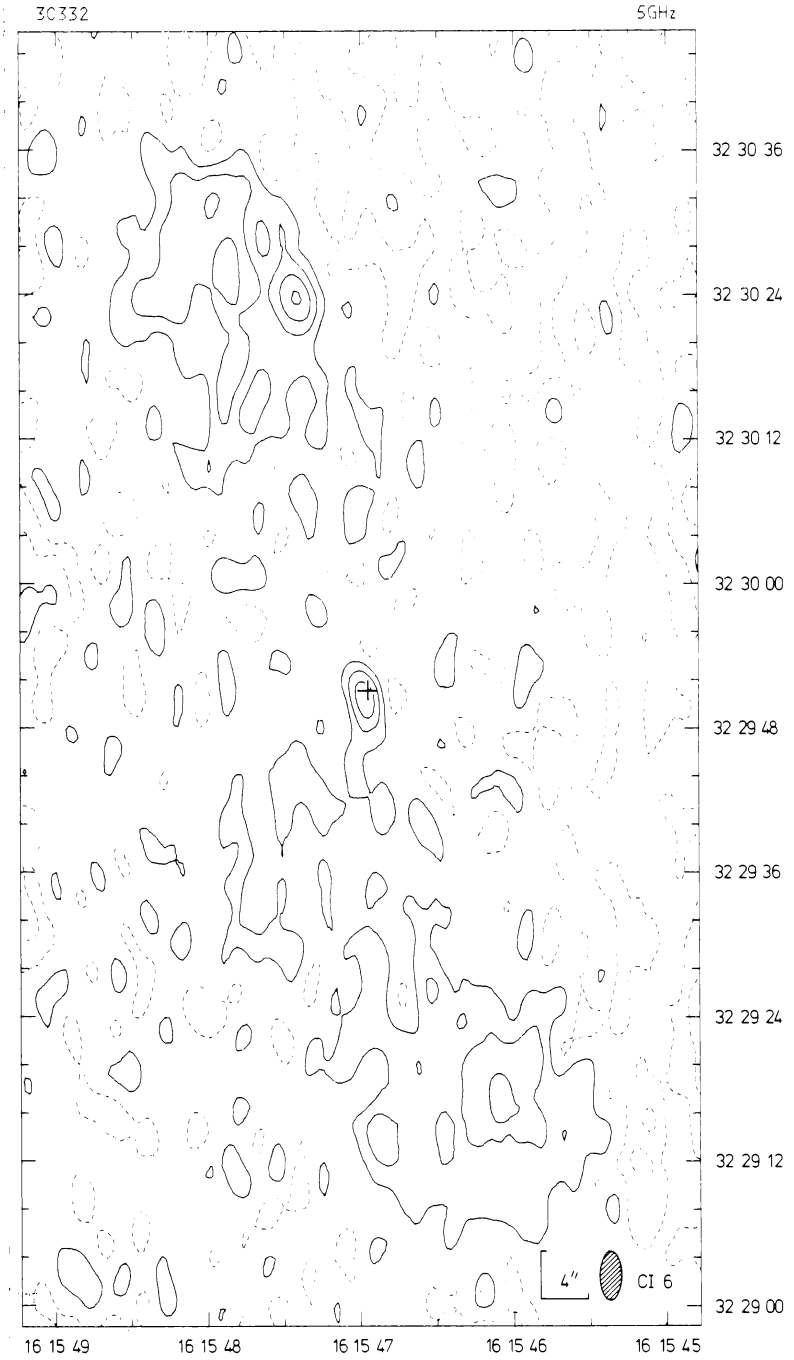

FIG. 15. 3C 332. *The cross marks a* 16^m *galaxy in a group.*

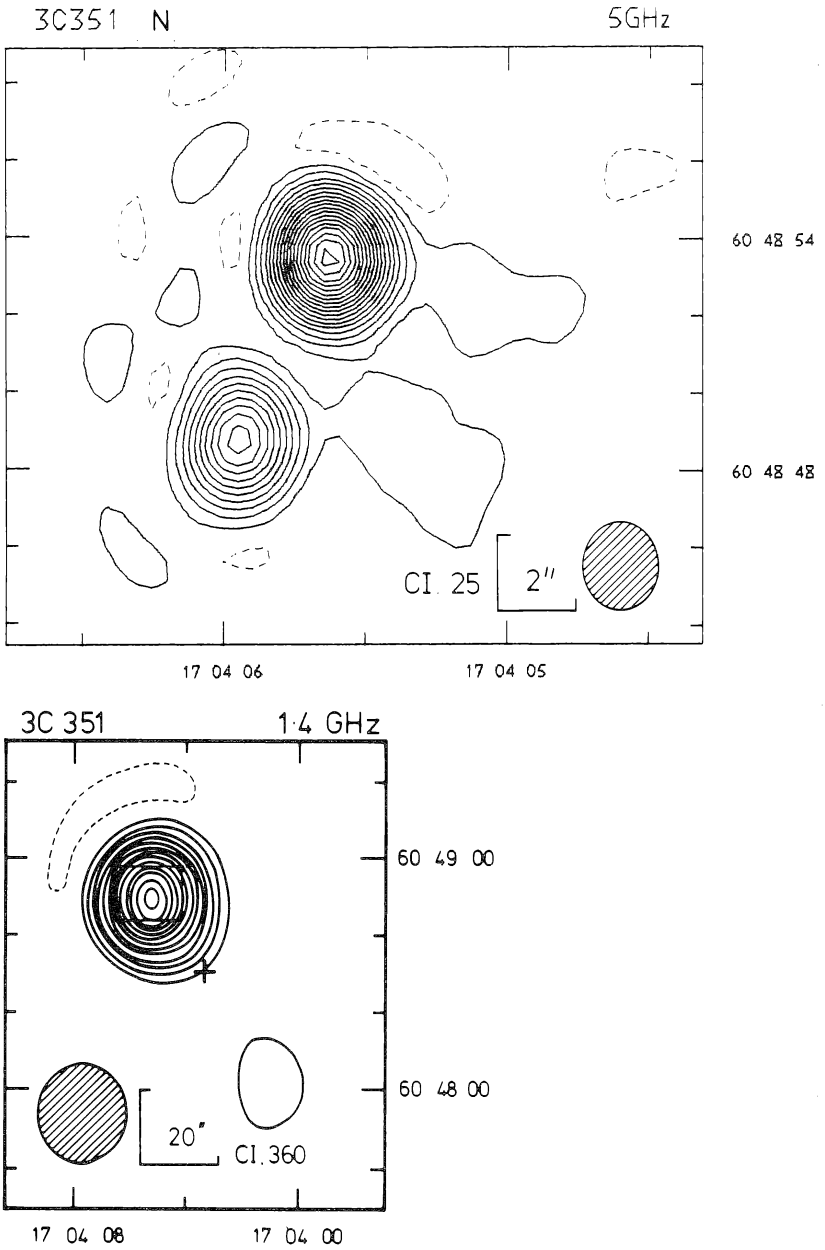

FIG. 16. *3C 351. The low resolution map at 1·4 GHz, from Mackay* (1969), *shows the very weak southern component. The high resolution map is of the northern component which itself shows double structure, in agreement with the results of Wilkinson, Richards & Bowden* (1974). *A further very weak component was found coincident with the* 15^m *quasar. The optical position of the quasar has also been measured by Barbieri, Capaccioli & Pinto* (1970).

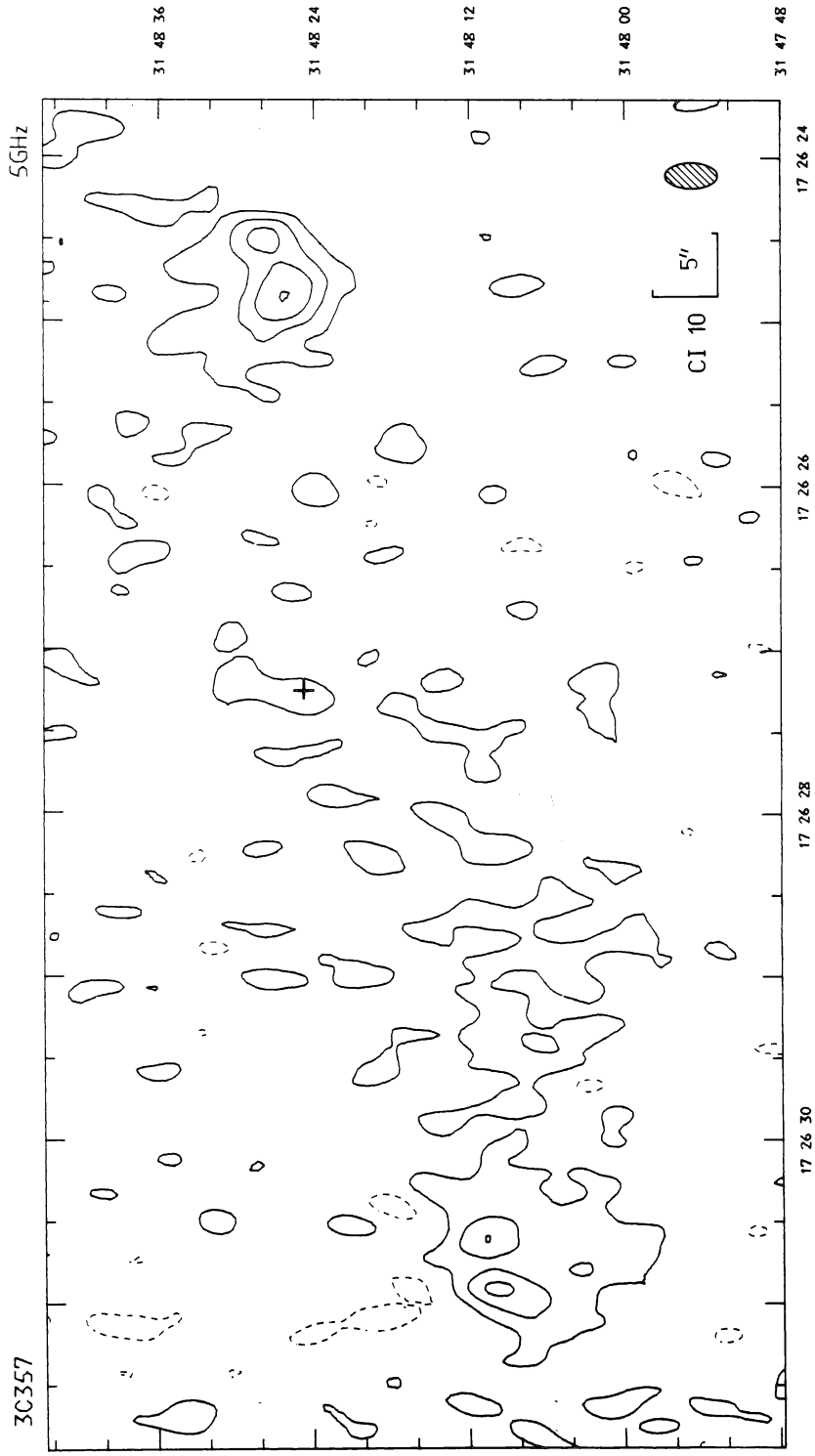

FIG. 17. 3C 357. *The cross marks a* 16^m *galaxy in a group.*

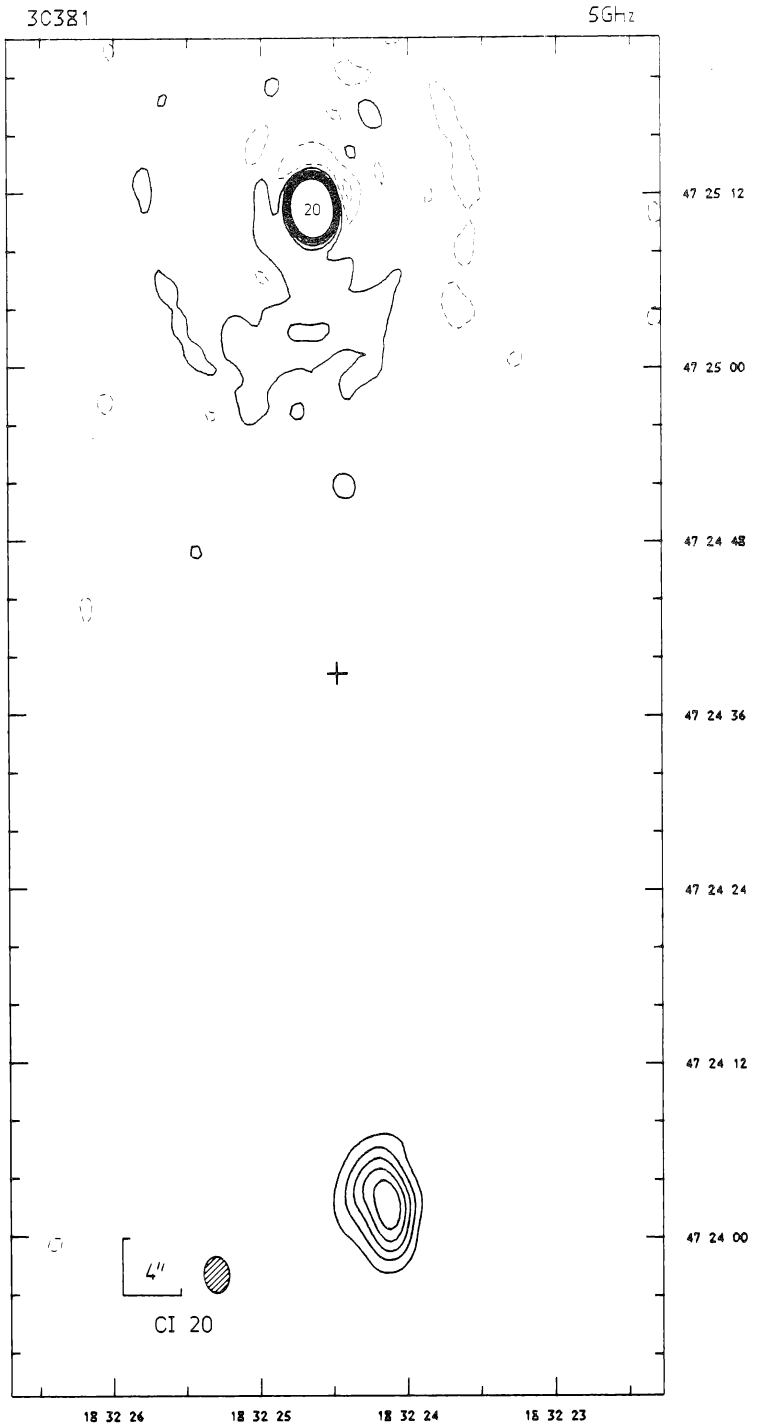

FIG. 18. 3C 381. *The cross marks an* 18^m *galaxy.*

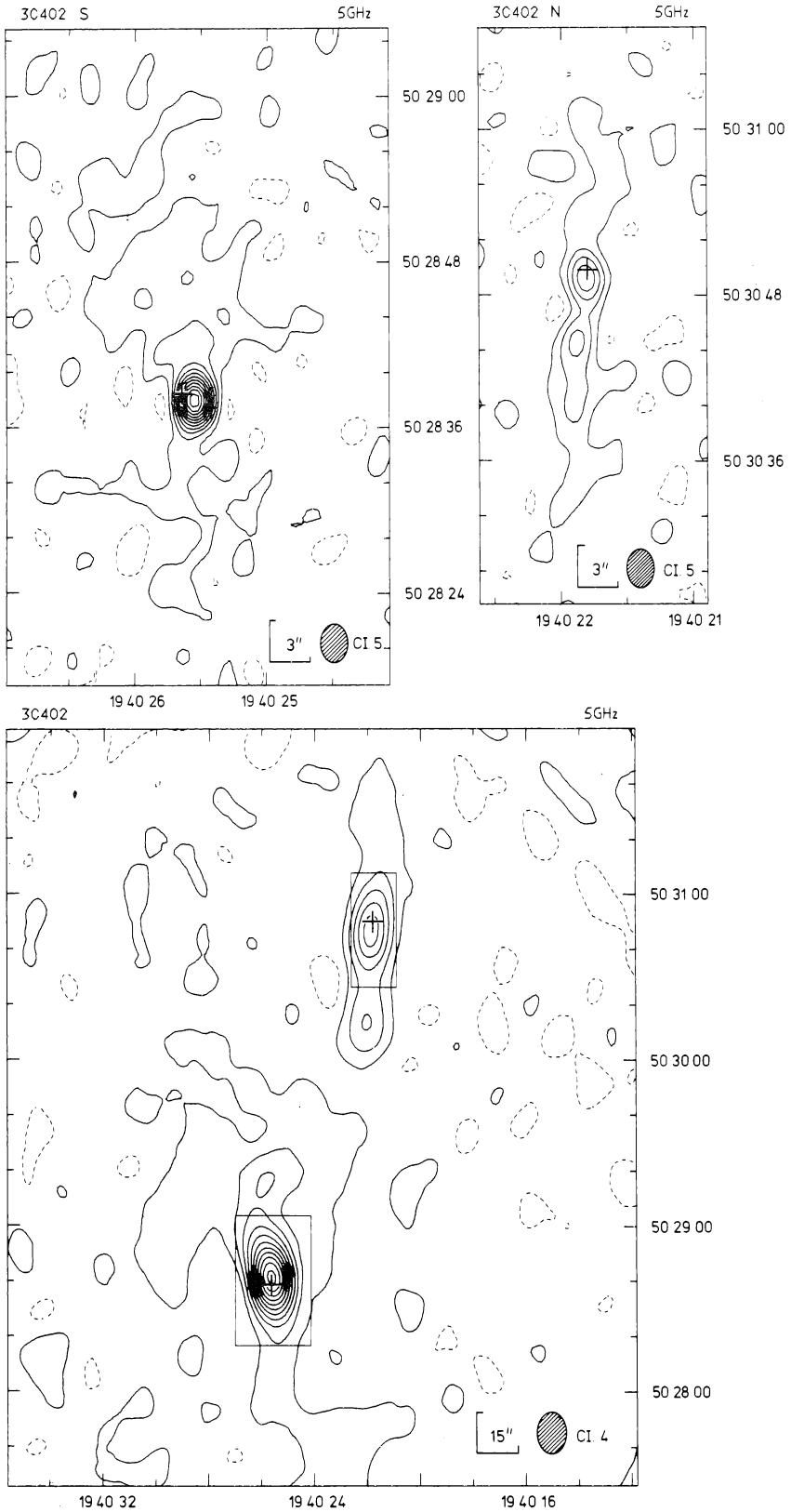

FIG. 19. 3C 402. *The large map has been smoothed to a resolution of 11″ × 15″. The two high resolution maps show the regions around the two bright galaxies, whose positions are marked. A further very faint component to the north was not detected here; see MKN.*

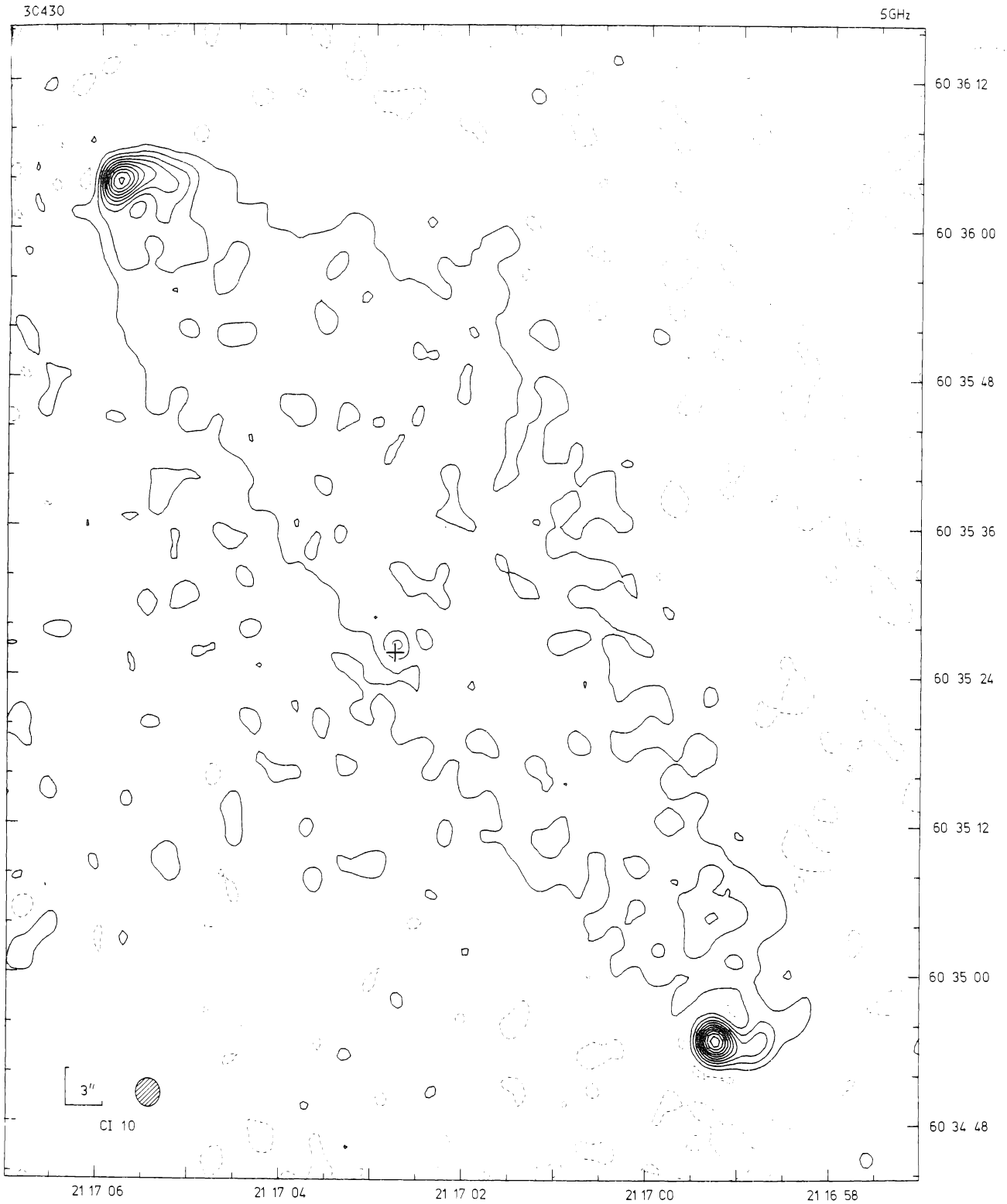

FIG. 20. 3*C* 430. *The cross marks the position of a* 15^m *elliptical galaxy coincident with a compact radio component.*

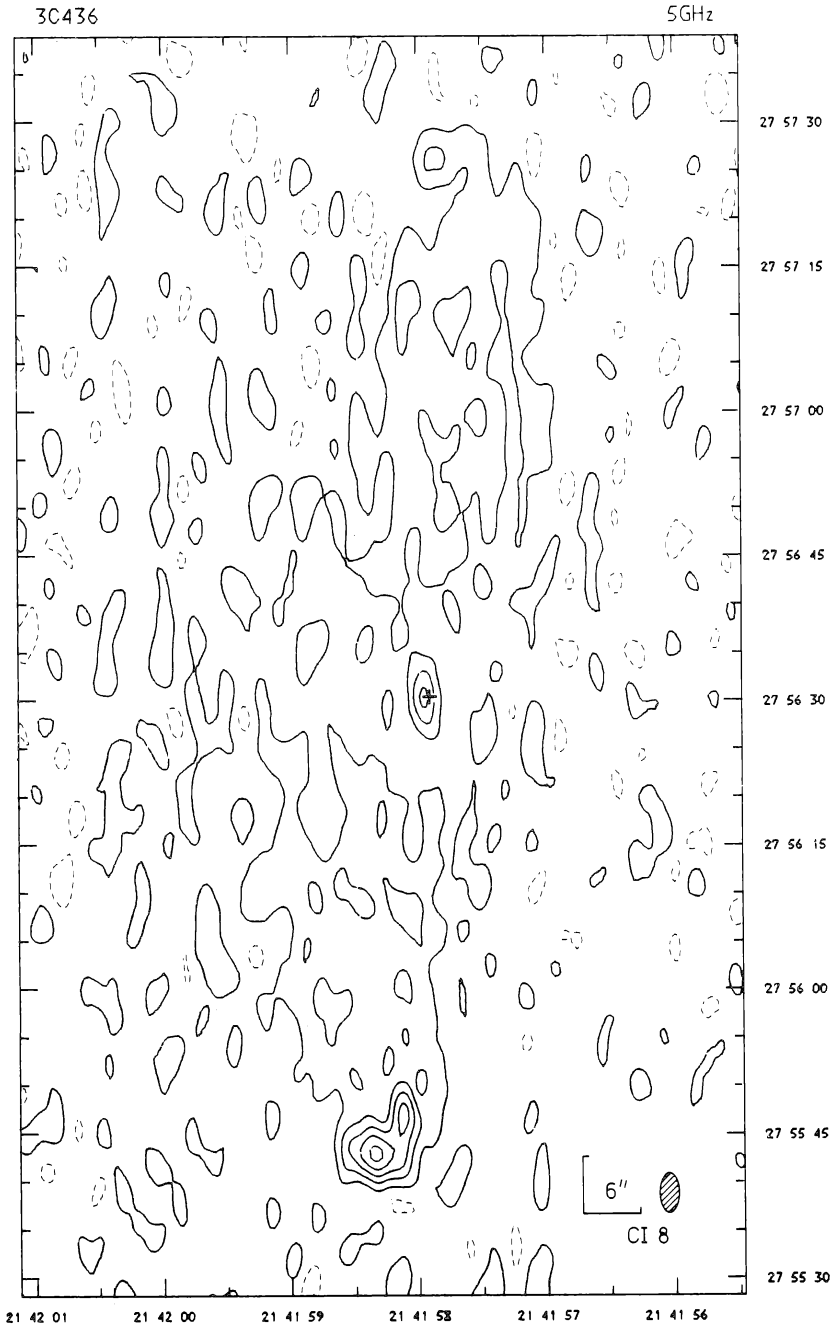

FIG. 21. 3C 436. *The cross marks the position of a* 19^m *galaxy.*

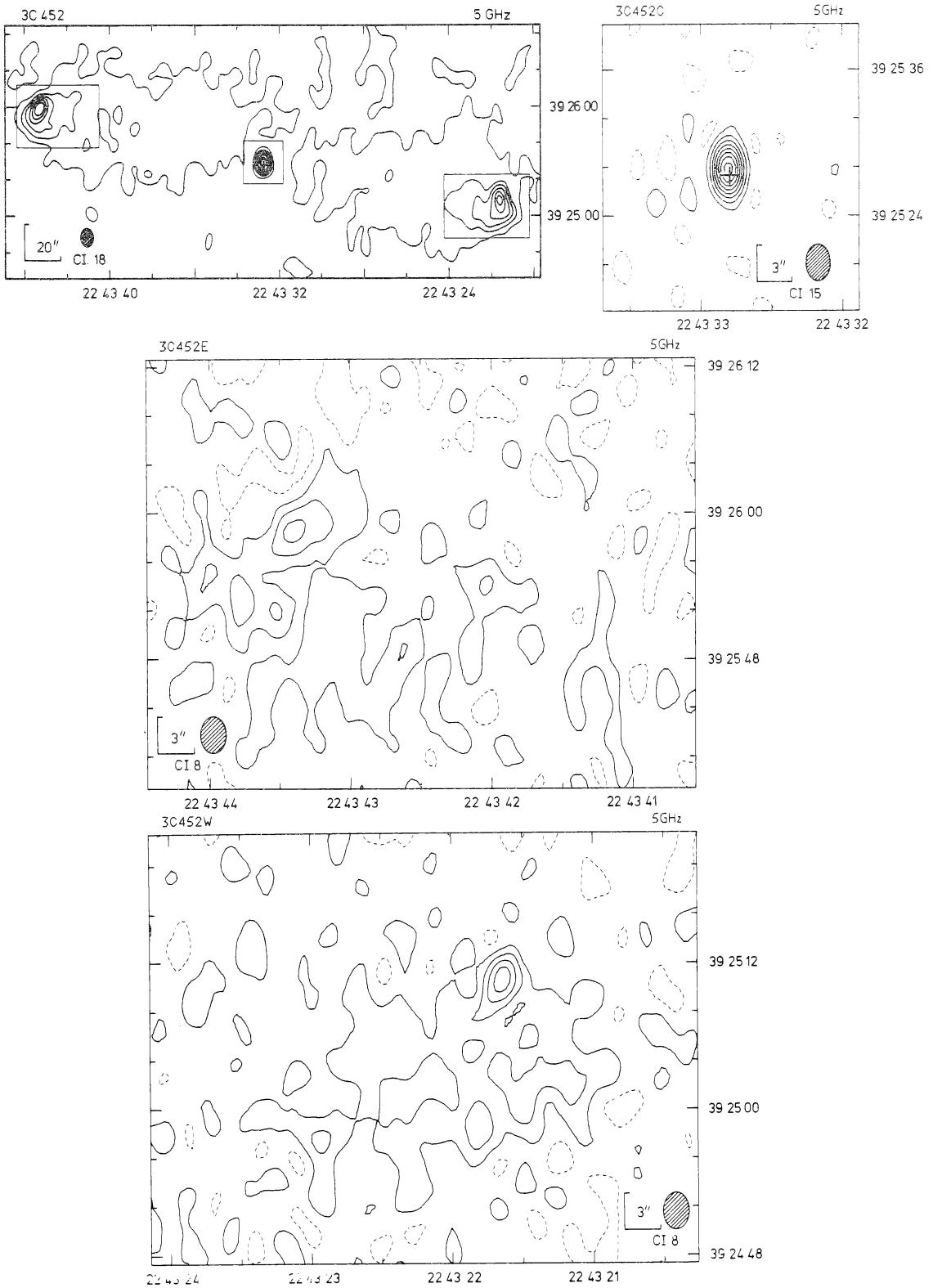

FIG. 22. 3*C* 452. *The lower resolution map* (6″ × 9″) *shows the overall structure at* 5 *GHz* (*Riley & Branson* 1973). *The three smaller maps have a resolution* 2″ × 3″. *The central components coincides with a* 16^m *galaxy.*

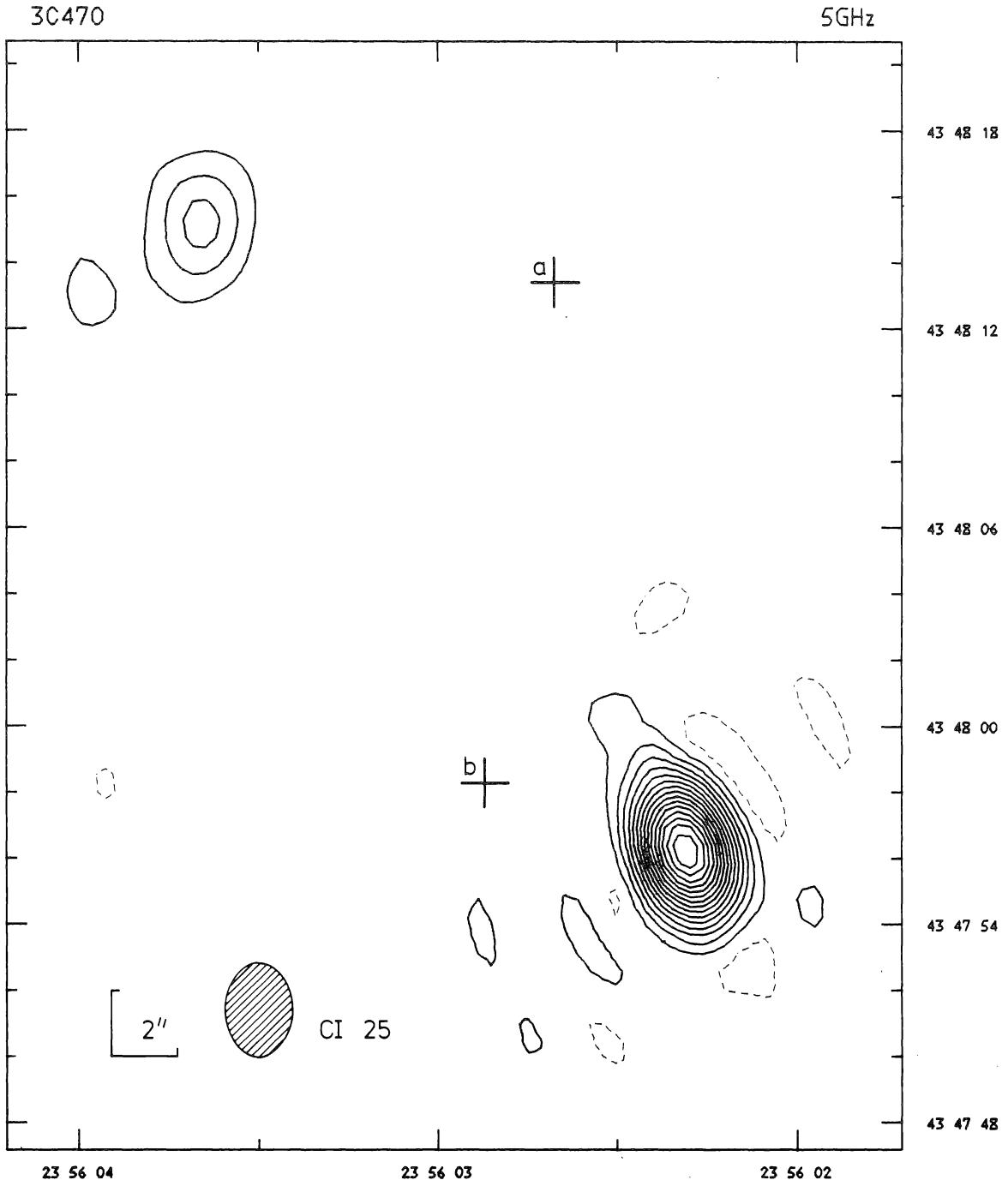

FIG. 23. *3C 470. The objects marked are (a) 19^m neutral object, and (b) 20^m red object. Neither appears likely to be related to the source.*

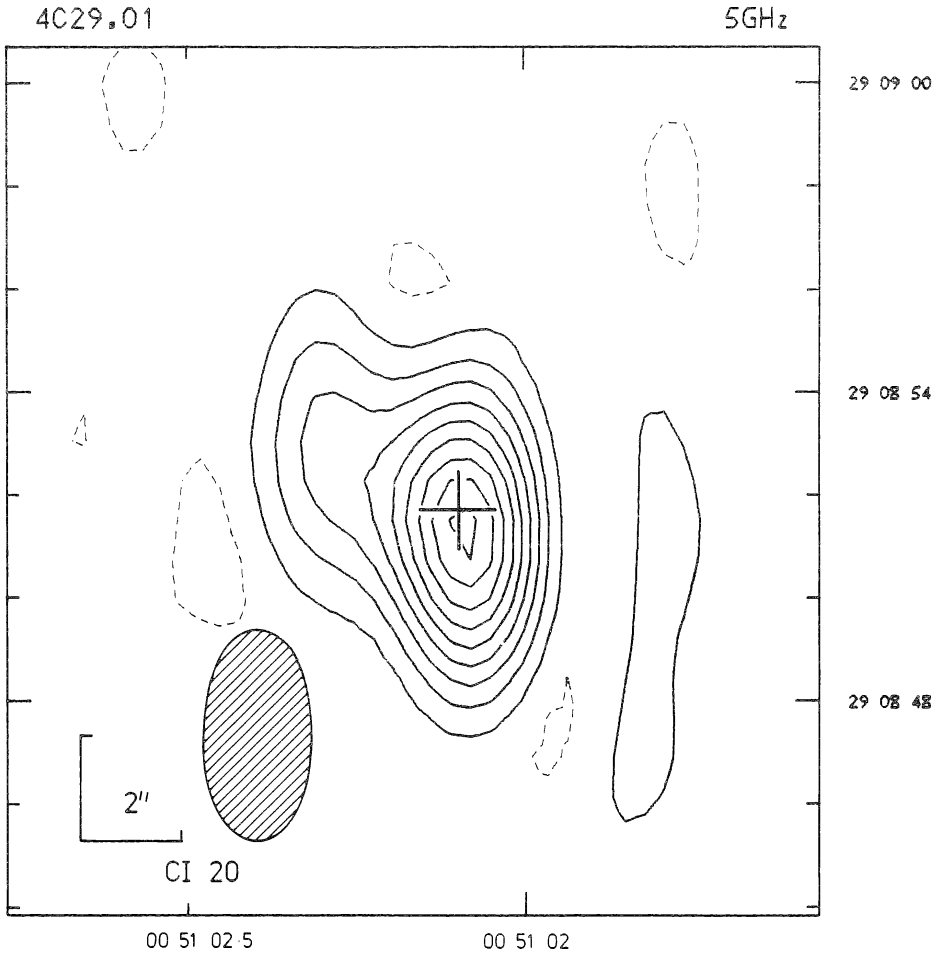

FIG. 24. 4*C* 29.01. *The cross marks an* 18^m *quasar with* $z = 1{\cdot}828$.

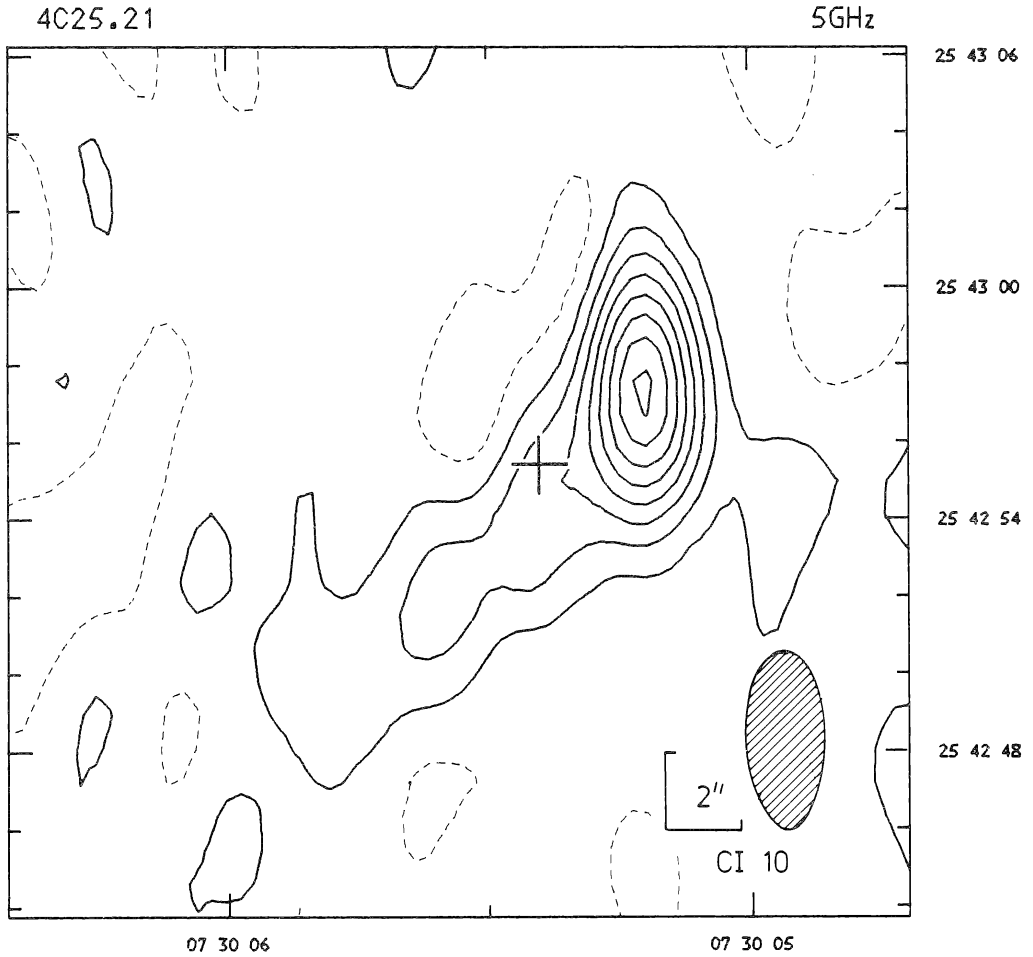

FIG. 25. 4C 25.21. *The cross marks a* 20^m *quasar with* $z = 2{\cdot}686$.

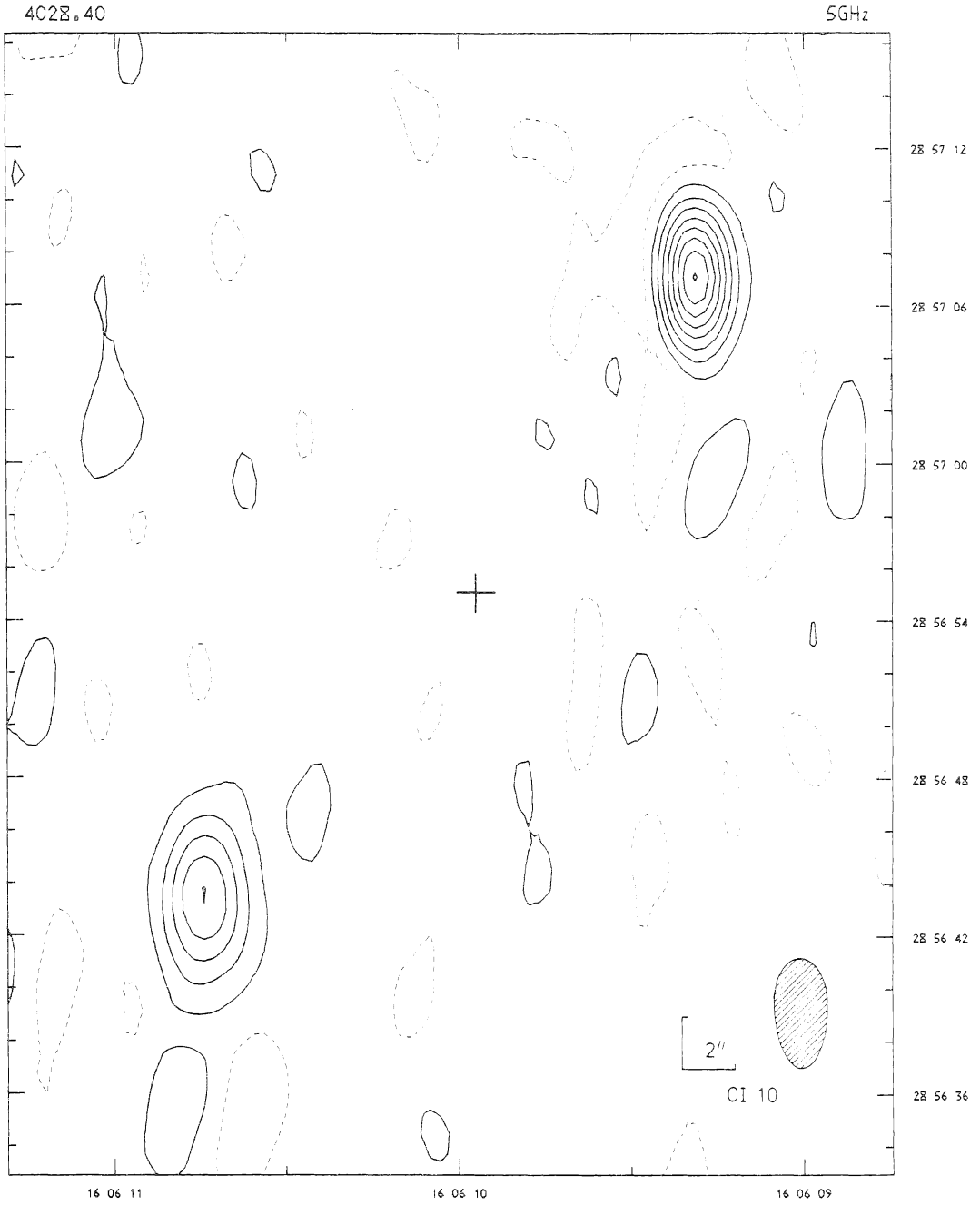

FIG. 26. 4C 28.40. *The cross marks a* 19^m *quasar with* $z = 1{\cdot}989$.